Particle Accelerators, 1971, Vol. 2, pp. 77–104

EXPERIMENTAL SHIELDING STUDIES AT HIGH-ENERGY PROTON ACCELERATORS — A REVIEW

H. WADE PATTERSON AND RALPH H. THOMAS

Lawrence Radiation Laboratory, University of California, Berkeley, California USA

'The ultimate result of shielding men from the effects of folly is to fill the world with fools.'

Herbert Spencer, *Essay* 1891

Progress during the past ten years in understanding the development of nuclear cascades in matter and its application to high-energy proton-accelerator shielding are described.

1. INTRODUCTION

Whatever the 'swinging sixties' may have meant for some, it represents a decade of steady and significant progress in the study and understanding of radiation shielding phenomena at high-energy accelerators.

Shortly after World War II, when extensive nuclear physics research was resumed, several new accelerators were designed and constructed. Rotblat,[1] in reviewing the progress of the 350-MeV synchrocyclotron at Liverpool, England, has described the fundamental lack of knowledge of the radiation fields produced by these instruments. He stated that this lack of basic knowledge of both the biological effects and the nuclear interactions of high-energy particles made it impossible to design effective radiation shields at that time. Two alternative solutions to this dilemma were adopted, both having their own advantages and disadvantages. Several synchrocyclotrons were constructed underground with substantial earth shielding overhead, both for the accelerator proper and for its associated experimental areas. Examples of underground accelerators are the 350-MeV synchrocyclotron at Chicago and the 110-inch synchrocyclotron at Harwell.[2] Such a solution had the advantage of eliminating any problems of excessive radiation external to the shield, and although costly, was not excessively so, because of the rather small physical size of the machines. However, such a solution was only short term—it could not be adopted indefinitely as accelerators grew in physical size, energy, and intensity. Furthermore, the absence of any radiation problem tended to inhibit undertaking fundamental studies leading toward efficient shield design.

At some laboratories, for example at the Lawrence Radiation Laboratory-Berkeley,[3] accelerators were built above ground level with minimal shielding in place. It was anticipated that as these accelerators were developed, beam energy and intensity would increase, although inadequate information initially precluded the design of an economical and efficient radiation shield. At such laboratories it was intended that radiation studies would form an integral part of the accelerator development program. Although the presence of continuing and increasing radiation problems at many of the first-generation accelerators has been a great stimulus for the improvement in our knowledge of shielding, such a policy also has considerable disadvantages. Lofgren[4] summarized his views, at a symposium organized at New York by the USAEC in 1957 to discuss the mounting radiation problem at accelerators, thus:

'I hope that the Cosmotron and the Bevatron are the last two large accelerators to be designed without shielding. I might mention a few of the varied problems from our experience when shielding is left as an afterthought.

'1. Shielding foundation had to be put in after the machine was completed, and this resulted in a serious interference with operation.

'2. Financing was inadequate because it was not planned long enough in advance.

'3. Many components that were installed in areas of high radiation level requiring shutdown for servicing might otherwise have been installed in low-level areas.

'4. In some areas it was nearly impossible to design a really good shield and also have access holes in the shield.

'5. It was necessary to abandon an appreciable area in the building which might have been used for laboratories and offices.'

The economic and operational inefficiencies resulting from incomplete consideration of radiation problems were documented at the New York symposium, and it paved the way for extensive studies of accelerator radiation fields in a more fundamental sense than hitherto. It was realized that the mere technical solution of particular problems did not facilitate extrapolation to new and unfamiliar situations. Falk,[5] in his introduction to the New York symposium, suggested that if shielding design were handicapped by the lack of available high-energy particle-interaction data then experiments should be performed to remedy this. He also drew attention to the fact that much available data did not find its way into the technical literature. In the sixties both of these deficiencies have been remedied. Substantial experiments to study radiation problems in a fundamental way have been mounted at several high-energy laboratories in the general spirit of a recommendation made in 1966 by a European Committee for Future Accelerators Working Group:

'The calculation of shielding for the accelerator and experimental areas, and the design of access tunnels depends, among other things, on knowledge of both transverse and longitudinal attenuation lengths, buildup factors, dose spectrum outside thick shields, and radiation attenuation in the tunnels. Present information on these factors is generally unsatisfactory and inadequate. The Working Group felt strongly that more reliable information would help to avoid the need for a high degree of conservatism in shielding design, and could certainly lead to significant cost reductions. Therefore, it is recommended that experiments on an adequate scale be carried out in the near future, for example at CERN, to improve present information. The Working Group wishes to emphasize the vital importance and urgency of these experiments. They should have at least as high a priority as normal physics experiments, with opportunity for data interpretation between runs to guide the course of work.'[6]

Progress in this field has been principally documented in the proceedings of several international conferences—the first organized in Paris in January 1962,[7] followed by others at Brookhaven, 1965,[8] Berkeley, 1967,[9] Chilton (Harwell), 1969,[10] and, most recently, Stanford, 1969.[11] Reviews on general aspects by Lindenbaum,[12] Livingston and Blewett,[13] and Ladu,[14] on dosimetry by Cowan[15] and Baarli,[16] on induced activity by Barbier,[17] and on shielding in the *Engineering Compendium on Radiation Shielding*,[18] fill in many specific details.

The problem was heightened not only by the operational experience described at New York, but also by the fact that several large accelerators around the world were either in the advanced design stage or under construction and would be operating at increased beam intensities or energies (or both) in the early sixties. In the middle sixties design studies for proton synchrotrons in the several-hundred-GeV region at Berkeley[19] and CERN,[20] high-intensity linear accelerators close to 1 GeV in energy at Yale[21] and Los Alamos,[22] and finally improvement programs to the Brookhaven AGS[23] and CERN PS led to important advances in our knowledge of accelerator radiation phenomena. The successful operation of the 70-GeV proton synchrotron at Serpukhov is already yielding new information,[24] and we now look forward to the experience to be gained at the National Accelerator Laboratory, Batavia, with operation at 200 GeV predicted in less than a year's time.

The radiation environment of an accelerator is *initially* determined by its beam characteristics. Beam losses during acceleration or beam transport to experiments, as well as beam use for experiments, all initiate the generation of nuclear cascades in accelerator components and shielding. This results in the 'prompt' radiation field that is present only when the accelerator is operating.

Physical understanding of the production of this nuclear cascade and its transmission through the accelerator shield provides the key to a sucessful solution of accelerator radiation problems. The attenuation of the nuclear cascade determines the quantity of shielding, and the composition of the nuclear cascade at deep depths determines the biological potency of the leakage radiation. Historically, attention was first given to the study of transmission of the nuclear cascade.

As induced activity and radiation damage from the interaction of the components of the nuclear cascade became severe they became matters of attention, but only relatively recently has any serious attempt been made to study the prime cause of accelerator beam losses. It seems clear that the old adage 'prevention is better than cure' is taken seriously only when it has to be necessity is truly the mother of invention!

The problems that engage the attention of the radiation physicist at a modern high-energy accelerator are thus many and varied. In addition to studying the prime cause of radiation fields he

must understand their transmission and transformation through shielding. The measurement and evaluation of accelerator radiation environments, which itself 'came of age' in the sixties, is a subject to which a lengthy review article could well be devoted. In this paper space has limited us to a discussion of the principal experiments made in the past 10 years and the increasing sophistication they have produced in our understanding of shielding performance. The increasing augmentation of our knowledge by neutron-transport calculations is only hinted at, and no detailed discussion of the practical aspects of accelerator shielding design is attempted. Several examples of practical shielding design, however, will be found in the literature referred to in this review, particularly the newly published *Engineering Compendium on Radiation Shielding*.[18]

2. HISTORICAL BACKGROUND

By 1960 Lindenbaum[12] and Moyer[25] had suggested the 'lines of attack' for the solution to the problem of shielding proton accelerators from several hundred MeV to several GeV. The qualitative features of the nuclear cascade induced by high-energy nucleons were understood and the concepts of particle buildup and equilibrium developed, and by utilizing data from several sources (cosmic ray data, nucleon-nucleus cross section data, the Metropolis[26] intranuclear cascade calculations, and shielding data), it was possible to make quantitative estimates of shielding. The collision of a high-energy nucleon with a nucleus gives rise to a large number of particles, principally nucleons, pions, and kaons, However, a substantial fraction of the incident energy may be vested in a single nucleon, which in crude terms may be thought of as propagating the cascade. At high energies, about 1 GeV, something like 20 to 30 per cent of the primary energy is radiated as pions,[27] but since their production spectra fall steeply with increasing energy, they do not play an important part in the cascade penetration. At deep depths in the shield neutrons take on the dominant role in cascade propagation, because energy loss becomes significant for protons and pions below about 450 MeV (where the ionization range becomes roughly equal to the interaction length).

Although pions (and kaons, which are produced only about one tenth as frequently) have little influence on the propagation of the nuclear cascade, their decay products, the muons, which have no strong interaction, form a very penetrating radiation—which will be of great importance at future high-energy accelerators.[28]

Early experimental studies of neutron attenuation at 90 and 270 MeV in a variety of materials and for poor-geometry conditions have been reported by Moyer and his colleagues.[3, 27, 30] Patterson also reported a measurement in concrete alone at 4.5 GeV.[30] Patterson[30] has interpreted the Berkeley experimental data in terms of an attenuation cross section, σ_a, analogous to the 'removal cross section' used in reactor physics.[31] He writes the attenuation cross section $\sigma_a(E)$ as a function of energy,

$$\sigma_a(E) = f(E)\sigma_{\text{tot}}(E), \tag{1}$$

where $\sigma_{\text{tot}}(E)$ is the total cross section at neutron energy E, and $f(E)$ is an arbitrary parameter related to the total cross section (and is given in Table I for concrete).

TABLE I

Values of $f(E)$ for concrete. (After Patterson).

Neutron energy (MeV)	$f(E)$
1	1.00
5	0.65
14	0.55
$\geqslant 150$	0.50

Figure 1 shows half-value thicknesses, calculated by using this prescription, compared with measurements at 90 MeV, 270 MeV, and 4.5 GeV in concrete. The general agreement between calculated and measured values is seen to be quite good, but the basic experimental technique was limited in these measurements to poor-geometry conditions. Lindenbaum[12] has explained such observations in terms of the inelastic cross sections:

'. . . Below 100 MeV the neutron inelastic cross section increases rapidly with decreasing energy until $E < 25$ MeV where in most cases the neutron inelastic cross sections level off and then decrease suddenly as shown in Fig. 2. . . . The increasing inelastic neutron cross section with decreasing energy in the region $25\ \text{MeV} \leq E_n \lesssim 100\ \text{MeV}$ means that neutron secondaries of high-energy primaries in this energy range reach an equilibrium buildup factor relative to the long-range primary component which controls the attenuation. For $E > 100$ MeV the secondary neutrons may still have an effectively shorter mean free path than a

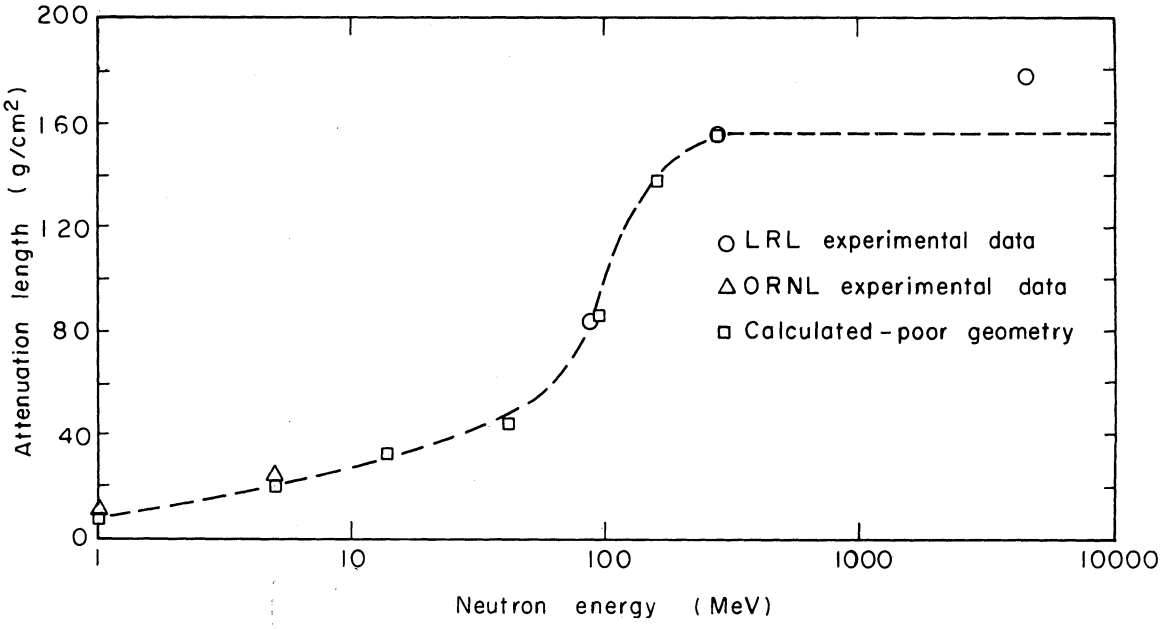

FIG. 1. Comparison between calculated and measured values of half-value thickness in concrete for neutrons. (After Patterson.)

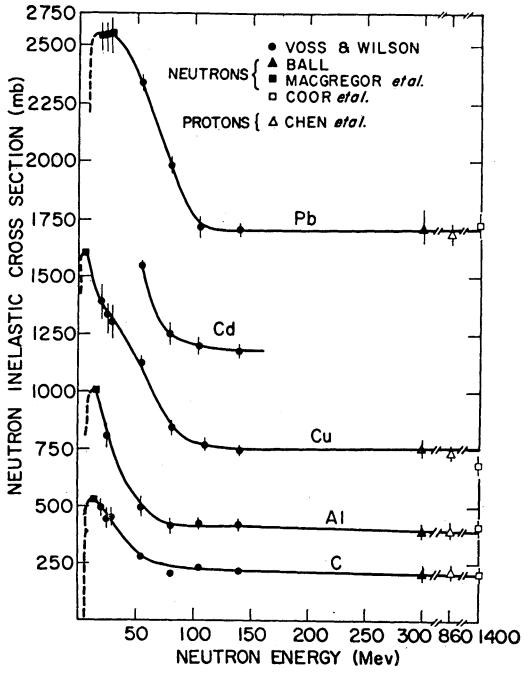

FIG. 2. Inelastic neutron cross sections as a function of energy in the range 0 to 1.4 GeV. (After Lindenbaum.)

higher-energy secondary, even though the inelastic cross sections are about the same, because of the increasing angular divergence with decreasing energy of the secondaries. It is these facts which tend to make high-energy ($E <$ several hundred MeV to several BeV) nucleon beams attenuate approximately exponentially (after a sufficient transition region) with a mean free path which is not very sensitive to the initial energy and is not much longer than the geometric mean free path calculated from the inelastic cross sections of the elements in the shield.'

Thus a qualitative understanding of the nuclear cascade is obtained in terms of the high-energy neutron interaction lengths and low-energy particle buildup. High-energy neutrons regenerate the cascade but are present in relatively small numbers. The radiation field observed at the interface of a shield consists of these high-energy 'propagators' born deep in the shield, accompanied by a train of 'camp followers' of much lower energy produced close to the shield surface. These lower-energy particles are directly produced in the intranuclear cascade or in the subsequent de-excitation of the struck nucleus by evaporation. Moyer[25] estimated the radiation accompanying each surviving 6-GeV nucleus in his calculation of Bevatron shielding—his results are given in Table II.

Although such buildup factors permitted crude

TABLE II

Estimated radiation accompanying each surviving 6-BeV nucleon. (After Moyer.)

Protons (from cascade and evaporation)	4
Charged pions	3
Muons	0.3
Neutrons (from cascade and evaporation in original star plus equal number from secondary collisions	7
Slow neutrons	70
Electrons (from π^0 decay and Compton scattering of capture γ rays and nuclear γ rays.	10 (?)
γ Rays: Enough to yield ionization dose of 3×10^{-4} mrem	

estimates of dose rate at a shield surface, precise details of particle spectra were of course of much greater value. Thomas[32] and Tardy-Joubert[33] made estimates of neutron spectra developed in accelerator shielding, assuming similarity at higher energies to the Hess cosmic-ray spectrum.[33, 34] Experimental techniques have been developed capable of measuring such spectra,[35] and their conversion to dose rate is now well understood.[36] These developments in the past 5 years have led to extremely important improvements in the accuracy of shield design.

The most vital step forward, however, has been the steady improvement in the design of experiments to measure attenuation length.

Thomas[38] has reviewed the measurements of attenuation length at high energies published up to mid-1964, and has reported values in steel ranging from 119 ± 10 to 179 ± 12 g/cm^2 and in concrete ranging from 108 ± 20 to 172 g/cm^2. These wide variations are principally due to differences in experimental technique, but also in part to different interpretations of the term 'attenuation length.' Following the arguments of Patterson and Lindenbaum, we might expect that at high energies

$$\lambda_{\text{atten}} \approx \frac{1}{N\sigma_{in}} \text{ cm}, \tag{2}$$

from which it follows that

$$\rho\lambda_{\text{atten}} = 38\, A^{1/3} \text{ g/cm}^2 \tag{3}$$

if the inelastic cross section is assumed to be geometric and the nucleon radius is taken as 1.2×10^{-13} cm. Keefe and Scolnick,[39] in reviewing experimental measurements of inelastic cross section, concluded that the best fit to the data is given by

$$\rho\lambda_{\text{atten}} = 38.5\, A^{0.31} \text{ g/cm}^2 \tag{4}$$

[not significantly different from the simple approximation represented by Eq. (3)].

Table III summarizes high-energy attenuation lengths calculated by Keefe and Scolnick, but it is clear that the early experiments reviewed by Thomas do not have sufficient precision to permit a meaningful comparison with the calculated values.

The evaluation of a precise attenuation length is of course a matter of great importance, since it is this parameter, above all others, that influences the radiation field transmitted by an accelerator shield. Considerable economies may be achieved at the larger accelerators if shielding need not be overdesigned. De Staebler,[40] in justifying his use of a large value of attenuation length in earth (170 g/cm^2), summarized the situation thus:

'It may appear that we are being unnecessarily conservative in taking the largest values of λ which have been measured, but the specter which haunts us in this connection is the unknown contribution to the attenuation from scattering out.'

By similar reasoning shield designs for the 200 and 300 GeV accelerators at Berkeley[19] and CERN[22] used attenuation lengths that were perhaps longer than necessary, because of the uncertainty in available data in the early 1960's.

A step of great importance in ordering understanding of the input parameters necessary to perform accurate shielding calculations was taken by Moyer[40, 41] in his work at the Bevatron. Based on experience at the Berkeley accelerators,

TABLE III

High energy mean free paths. (After Keefe and Scolnick.)

Element	A	ρ (g/cm^3)	σ_a (mb)	Removal mean free path (g/cm^2)	(cm)
C	12.01	2.25	240	83.2	37.2
Al	26.98	2.7	417	107	39.7
Fe	55.85	7.7	688	134	17.4
Pb	207.19	11.9	1710	202	18.4
U	238.03	18.7	1870	210	11.2

Moyer developed a phenomenological model capable of estimating the additional shielding to be required as part of the Bevatron improvement program during 1962–63. Since first proposed by Moyer, this model has been developed somewhat further, and the interested reader is referred to the literature.[19, 40–45]

A proton accelerator may be considered, for the purpose of calculating shielding, as a source of neutrons. In the high-energy strong-focusing proton synchrotrons it is sufficiently accurate to ignore the radial curvature of the accelerator. Figure 3 shows a typical two-dimensional representation of the accelerator as a line source of neutrons of variable intensity.

The neutron flux density, ϕ, in n/cm^2 sec, at a point outside the shield and greater than some energy $E_{\min}$ is expressed as

$$\phi = \int_{-\infty}^{\infty} \int_{E_{\min}}^{E_{\max}} S(z)\, f(E,\theta)\, r^{-2} \cdot \exp\left(-\frac{\mathrm{d}\,\mathrm{cosec}\,\theta}{\lambda(E)}\right) B(E,\theta)\,\mathrm{d}E\,\mathrm{d}z, \qquad (5)$$

where a, d, r, and θ are explained by Fig. 3,

$S(z)\,\mathrm{d}z$	is the number of neutrons emitted in unit time by the line element between z and $z+\mathrm{d}z$,
$f(E,\theta)$	is the distribution of the neutrons emitted as a function of the energy and the angle, per steradian,
$E_{\min}$ and $E_{\max}$	represent the energy range of interest. In many cases $E_{\max}$ will be the maximum energy in the neutron spectrum and $E_{\min}$ will be the minimum neutron energy detected,
$\lambda(E)$	is the attenuation length of neutrons of energy E in the shield, and
$B(E,\theta)$	is the buildup factor as a function of the energy and the geometry.

The integration is carried over the appropriate limits of z—in this case for an infinite line source.

As we have seen, the attenuation length of neutrons increases with increasing energy up to about 150 MeV and remains approximately constant beyond that. After a few mean free paths of shielding, the nuclear cascade, generated by the slowing down of the high-energy neutrons through elastic and inelastic scattering, gives rise to the formation of an equilibrium spectrum whose attenuation is determined by the fast component above 150 MeV. This justifies the essential simplification made by Moyer in his calculational method to consider only neutrons above 150 MeV. We can then write

$$\lambda(E) \approx \lambda \qquad \int_{E_{\min}}^{E_{\max}} f(E,\theta)\,\mathrm{d}E \approx g(\theta), \qquad B(E,\theta) \approx 1, \qquad (6)$$

where $g(\theta)$ is the angular distribution of neutrons with more than 150-MeV energy. Hence the high energy flux is expressed as

$$\phi(E_n > 150\ \text{MeV}) = \int_{-\infty}^{\infty} S(z)\, g(\theta)\, r^{-2} \cdot \exp\left(-\frac{\mathrm{d}\,\mathrm{cosec}\,\theta}{\lambda}\right)\mathrm{d}z. \qquad (7)$$

Moyer took as a source the interaction of 6-GeV protons in a thick copper target ($\approx 100\ \text{g/cm}^2$), and then he wrote Eq. (7) for a point source in the form

$$\phi_p(E > 150\ \text{MeV}) = \frac{N\, g(\theta)}{(a+\mathrm{d})^2\,\mathrm{cosec}^2\theta} \cdot \exp\left(-\frac{\mathrm{d}\,\mathrm{cosec}\,\theta}{\lambda}\right), \qquad (8)$$

When a conversion factor appropriate to high-energy neutrons is selected, F neutrons cm^{-2} sec^{-1} mrem hh^{-1}, and particle equilibrium is assumed,

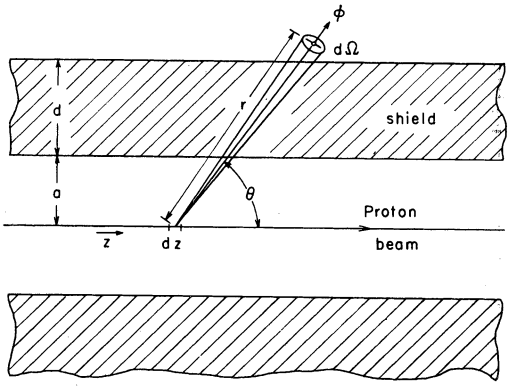

FIG. 3. Two-dimensional representation of shielding geometry for a large proton accelerator. (After Routti and Thomas.)

the dose-equivalent rate, DE_p is given by

$$DE_p = kF\phi_p(E > 150\ \text{MeV})$$
$$= \frac{kF\,Ng\,(\theta)}{(a+\text{d})^2\ \text{cosec}^2\theta} \exp - \frac{\text{d cosec}\ \theta}{\lambda} \quad (9)$$

where k is the ratio of the total dose rate in the spectrum to that due to particles greater than 150 MeV. In evaluating the parameters in Eq. (9) Moyer utilized cosmic ray data, the Monte Carlo calculation by Metropolis *et al.*,[26] and experimental data taken at the Bevatron.[46]

Moyer's shield calculations were designed to reduce neutron transmission by a factor of 100. Thomas[43] and Smith[47] have reviewed measurements taken at the Bevatron before and after the additional shielding was installed. These measurements show that the overall effect of the additional shielding was to reduce neutron flux levels by a factor between 90 and 100, the exact value depending upon neutron detector and location.

In the past 10 years the basic physical assumptions of the Moyer Model have been studied and found to be substantially supported by the experimental data. The concept of 'ray tracing' used by Moyer has proved to be valid at deep depths in shielding and when particle equilibrium is established. Values of attenuation length measured in carefully designed experiments are very close to those expected, and particle spectra may now be readily converted to dose rate. In consequence, particle accelerator shields may now be designed with an accuracy to within about a factor of two in radiation field at the shield surface.

Several experiments performed during the last 10 years have been of great importance in establishing this progress, and merit discussion in some detail. As shielding experiments progressed through the decade they became more sophisticated in design and ambitious in scope. An understanding of this development reveals the sources of confusion in earlier radiation studies.

3. CERN SHIELDING EXPERIMENTS, 1960–1963

Increasing pressure from groups actively engaged in accelerator design or construction for a resolution of the early uncertainties discussed above led to the performance of a series of shielding experiments at the CERN PS. It had become clear that two alternative approaches to solving the problem of scattering out were possible. The first was to use a very wide incident particle beam with large angular divergences and assume that 'scattering in' and 'scattering out' are balanced. The second approach was to use a narrow, parallel incident beam and to measure all the particles reaching a given depth in the absorber, either by using a large detector or by making particle-density profile scans. The latter alternative was adopted in the CERN experiments primarily because a narrow beam was more readily available, but also because inherently more information is available from such an experiment.

Four experiments were carried out at CERN in the period 1960–1963, which are summarized in Table IV.

TABLE IV

CERN shielding experiments, 1960–1963.

Experiment Number	Date	Incident proton energy (GeV)	Absorber density (g/cm^3)	Beam size[a]	Neutron contamination of primary beam	Attenuation length (g/cm^2)	Reference
1	1960	20–24	Concrete $\rho = 2.5, 3.6$ Earth $o = 2$	H: 25 cm[b] V: 8 cm[c]	48±5%	145±10	48, 49
2	1961	20	Concrete $\rho = 3.6$	H: 1.7 cm V: 6.2 cm	29±4%	132±5	48–50
3	1962	10	Concrete $\rho = 3.6$	H: 6 cm V: very wide	20±3%	164±20	49
4(a)	1962	10	Steel	H: 1 cm	25±5%	119±20	52
4(b)		20	$\rho = 7.8$	V: 1 cm	10±3%	137±10	53

a. Width at half intensity.
b. H means horizontal.
c. V means vertical.

Ilford G.5 nuclear emulsions were the principal detectors used through the entire CERN series of experiments. Scanning was carried out for both minimum-ionizing tracks and stars, providing the possibility of discriminating between nuclear active particles and muons at deep depths in the shield.

The final experiment in steel with 10- and 20-GeV/c protons (whose design is shown in Fig. 4) incorporated all the experience gleaned from its predecessors.[51] Neutron contamination of the primary proton beam was reduced by large bending of the secondary proton beam scattered from an internal target in the accelerator. Beam size (which at incidence was 1.2×1.2 cm) and divergence (± 2.1 mrad) were limited by two collimators in the beam transport system. Unwanted 'halo' around the incident beam and side scattering were reduced by concrete shielding around the steel assembly, which itself was sufficiently large in comparison with the beam dimensions to be regarded essentially as an infinite steel slab. Cavities in the steel in which detectors were placed were made as small as possible to reduce any perturbation of the nuclear cascade. Although not entirely successful in achieving all these goals, this final experiment in steel represented a great step forward in the design of shielding experiments and went a long way toward eliminating many of the extraneous factors that had influenced previous experiments and made their interpretation difficult. Since the measurements in steel are the most accurate of the series, we describe the results obtained in detail. Figure 5 shows typical beam-profile scans as a function of depth in steel, made with protons of incident momentum 10 GeV/c.[52] Similar results were obtained at 20 GeV[53] and are summarized in Fig. 6, which shows the full width at half intensity of such lateral distributions obtained from both track and star scanning. The linear increase in particle distribution with penetration is a qualitative indication that Moyer's concept of 'ray-tracing' high-energy particles through the absorber, described in the preceding section, is realistic. From such profiles the total number of particles crossing a plane perpendicular to the beam direction may be obtained by integration. Figure 7 shows such an integrated track intensity compared with the track intensity on the beam axis measured at 10 GeV/c. The slope of the peak intensity curve obtained was 119 ± 5 g/cm^2, compared with an estimate of $165 (\pm 30\%)$ g/cm^2 for the slope of integrated intensity. The difference between these two estimates of slope gives an indication of the influence of geometry on the results of attenuation measurements and, in large measure, explains the wide range reported in the literature. Although at 10 GeV/c no buildup on beam axis for either stars or tracks was observed in steel, at 20 GeV/c some small buildup was measured.[53] Integration of star and track profiles gave an asymptotic relaxation length of 185 ± 20 g/cm^2. Figure 8 shows star densities measured on and parallel to the beam axis (as a function of depth)[53] at 20 GeV/c. The

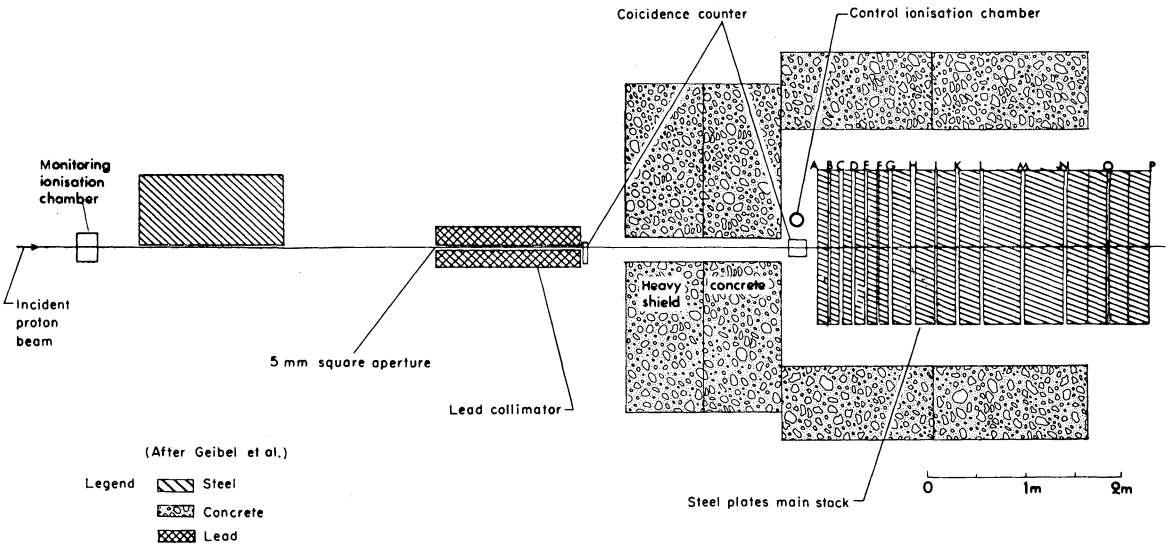

FIG. 4. Detailed experimental layout of CERN shielding experiment in steel. (After Geibel *et al.*)

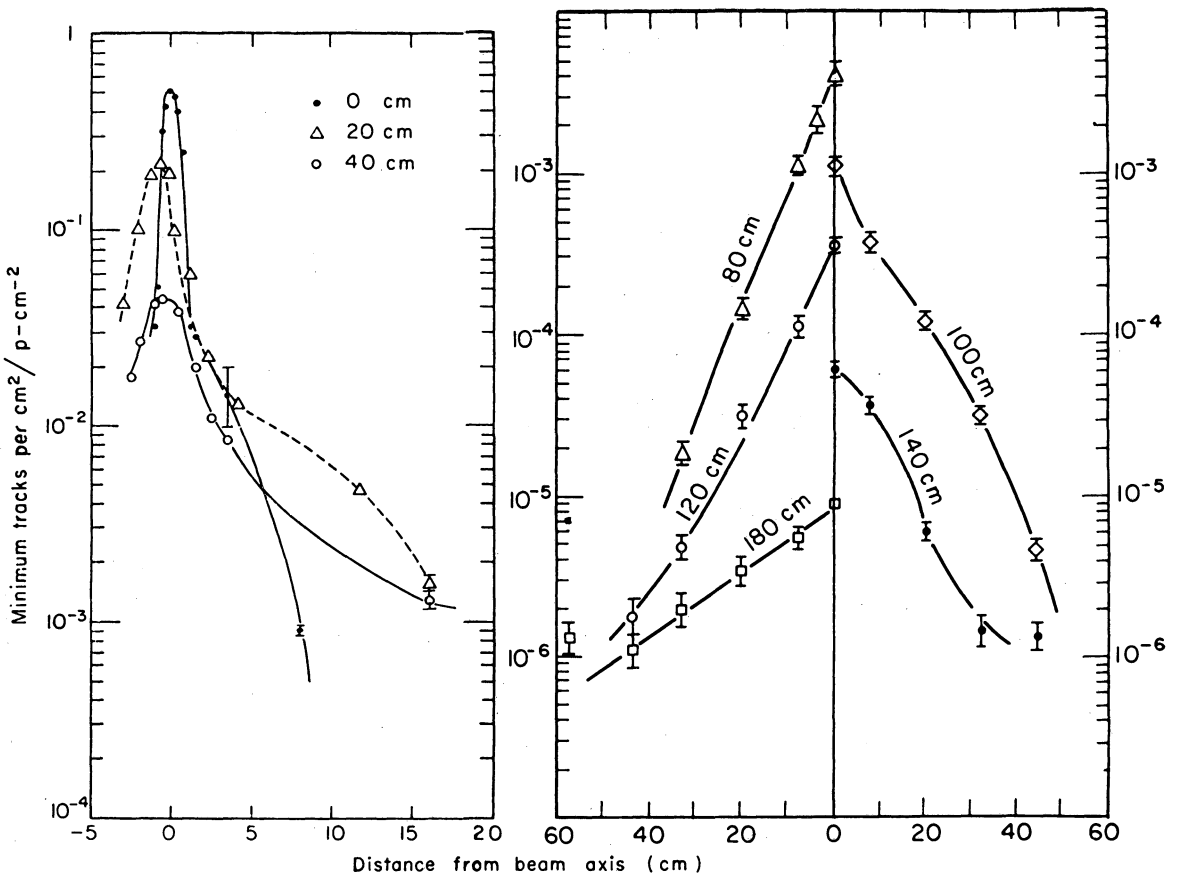

FIG. 5. Typical horizontal scans at beam height in steel as a function of depth (incident proton momentum 10 GeV/c). (After Childers *et al.*)

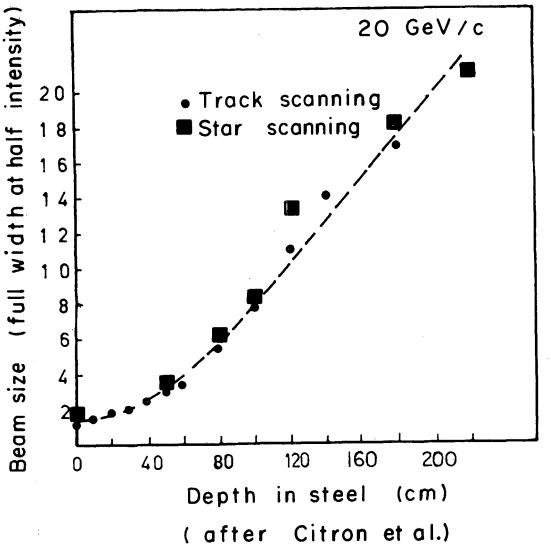

FIG. 6. Increase in width of high-energy-particle distribution in steel. Incident proton momentum 20 GeV/c. (After Citron *et al.* 1965.)

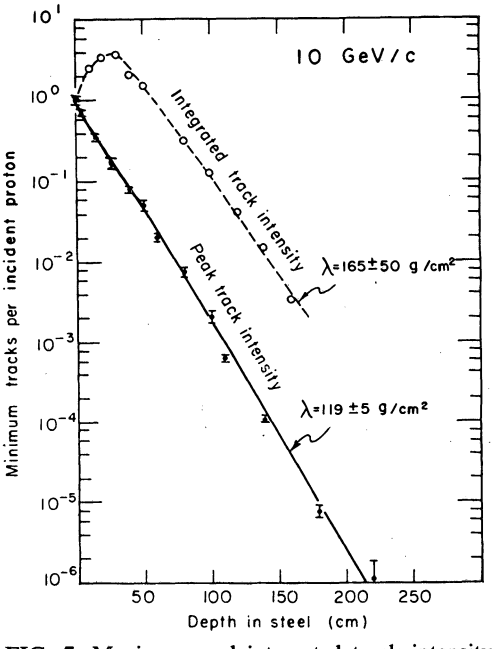

FIG. 7. Maximum and integrated track intensity as a function of depth in steel. Incident proton momentum 10 GeV/c. (After Childers *et al.*)

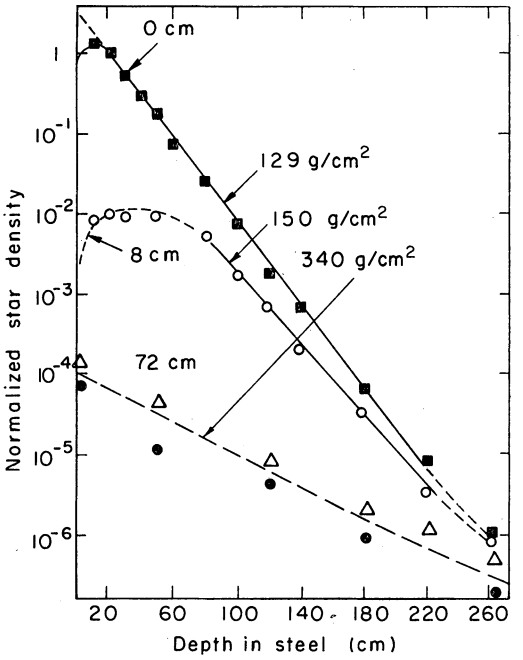

FIG. 8. Variation of star density as a function of depth in steel measured along the beam axis and parallel lines 8 cm and 72 cm from the axis. Incident proton momentum 20 GeV/c. (After Citron *et al.*)

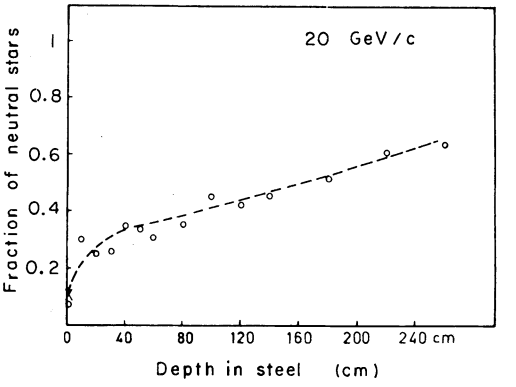

FIG. 9. Fraction of 'neutral' stars (i.e., with no charged primary in the backward hemisphere) as a function of depth in steel incident proton momentum 20 GeV/c. (After Citron *et al.*, 1965.)

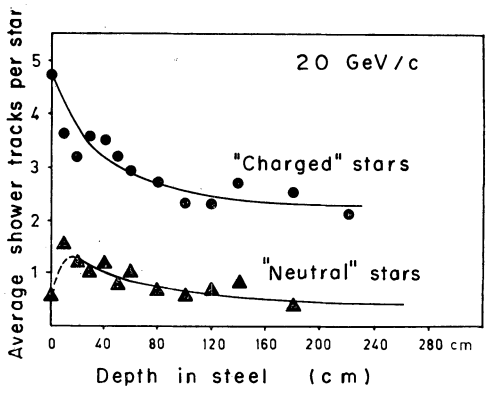

FIG. 10. Average number of shower (minimum ionizing) tracks emitted per star as a function of depth in steel. Incident proton momentum 20 GeV/c. (After Citron *et al.*, 1965.)

difficulty in defining a unique relaxation length is clearly demonstrated!

The use of nuclear emulsion permitted visual inspection of stars and hence a rough determination of whether they were produced by an uncharged or charged incident particle. Figure 9 shows the fraction of stars with no charged primary (judged by the absence of a minimum-ionizing particle in the backward hemisphere) measured for 20-GeV/c primary protons. The increasing fraction of stars created by neutrons is clearly seen; its steady increase probably indicates that an equilibrium ratio of high-energy protons to neutrons has not been completely established. Measurements at 10 GeV/c indicate a somewhat more rapid approach to equilibrium.[52]

Measurement of the average multiplicity of minimum-ionizing particles emitted from stars gives a rough indication of the average energy of the incident particles. Figure 10 shows that the average shower track number, $\bar{n}_s$, of stars produced by the interaction of charged primaries decreases rapidly with penetration into the steel. Thus at a depth of 100 cm in steel $\bar{n}_s$ is about 2.6, corresponding to an average energy of 6 GeV. The energy loss of 20-GeV protons in 100 cm of steel is about 1.6 GeV, therefore at this depth the uninteracted primary proton beam would have an energy of 18.4 GeV. This difference of about 12 GeV is of course due to energy transfer by nuclear interaction, and indicates that the charged particles initiating the stars deep in the steel have themselves originated from nuclear interactions.

In addition to nuclear emulsion, carbon threshold detectors and ionization chambers were used. Although limited by sensitivity and large detection size, these measurements confirmed a relaxation length of about 160 g/cm², both for absorbed dose and for particles greater than 20 MeV. Because of the large detector size relative to the beam, information on particle buildup is limited, but Baarli *et al.*[54] estimate a total of nine particles of

greater than 20 MeV to be produced by an incoming 20-GeV proton, which they consider to be in good agreement with the value of nine cascade nucleons per inelastic interaction at 3 GeV listed by Lindenbaum.[55] It is not completely clear, however, to what extent charged pions were detected in the experiment by Baarli *et al.*

Two groups have attempted to compare the experimental data obtained in the CERN series of shielding measurements.

The earlier experiments have been studied by Alsmiller *et al.*,[56–58] who solved the coupled cascade transport equations in 'straight-ahead' approximation and applied these results to the calculation of the components of a cascade generated in heavy concrete by 24-GeV protons.[58] Comparison of these calculations with the measurements at 20 and 24 GeV reported by Citron *et al.*[48] is difficult for several reasons. Citron *et al.* measured the nuclear star density on beam axis, whereas the one-dimensional Oak Ridge calculations should be compared to an integration over a plane transverse to the beam direction. Furthermore, the effective energy threshold of a star is somewhat ambiguous, depending upon scanning technique and efficiency, but is of the order of 100 MeV. Figure 11 shows a comparison between measured star density in the broad- and narrow-beam experiments and the calculated values for different production energy thresholds. The measured star densities are attenuated more rapidly than the calculations predict, as expected. Figure 12 compares the measured and calculated fractions of all stars produced by neutrons. Neutron contamination of the beam influences the experimental results.

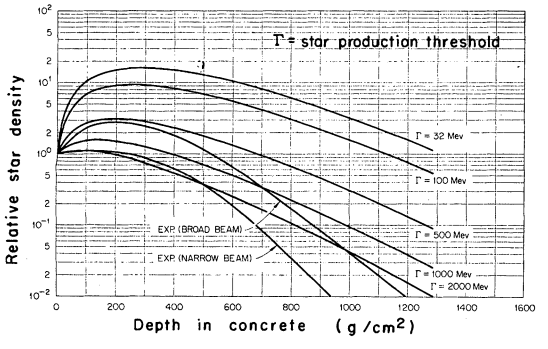

FIG. 11. Comparison of star densities calculated by a 'straight-ahead' model with experimental data in concrete. Incident proton energy 24 GeV. (After Alsmiller and Murphy.)

Geibel and Ranft[59] used a Monte Carlo method to estimate the three-dimensional development of the nuclear cascade induced in steel and obtained good agreement with the experimental data reported by Citron *et al.*[53] and Childers *et al.*[52] These early calculations were, however, limited by the secondary-particle production input data. Ranft[60] has now improved these data and repeated the calculations more precisely with improved secondary-particle production information. Figures 13 and 14 show typical results obtained indicating excellent agreement. Unfortunately, good as this agreement is, neither experimental nor theoretical techniques have yet reached the stage where direct overlap is possible. Numerical solutions of the coupled cascade transport equations in straight-ahead approximation, although accurate at high energies, become less and less reliable at low energies. Similarly, adequate particle-production information for input into Monte Carlo calculations is not yet available, and the results of such computations become increasingly suspect at lower secondary-particle energies.

4. BERKELEY SHIELDING EXPERIMENT—1964

The beam intensity available for the CERN experiments was limited to $\approx 10^5$ protons/sec. Measurements with nuclear emulsions were made down to relative transmissions of between 10^{-5} and 10^{-6}, but measurements with activation detectors and ionization chambers were limited to relative transmission of only 10^{-3}. Since secondary particles below 50 MeV in general produce the largest component to the dose equivalent outside shielding,[32] it is necessary to study their production and transmission through thick shields. The development of an extracted proton beam of much higher intensity at the Bevatron made it possible to design an experiment designed to fill in some of the unresolved details in the CERN series of experiments.

In 1964 an experiment was mounted at the Bevatron that used a 6.2-GeV proton beam of maximum intensity 10^{11} protons/sec. At the front face of the experimental array of concrete blocks the beam spot was circular and approximately 5 cm in diameter. The high incident beam intensity permitted measurements to depths of 24 ft in ordinary concrete (1760 g/cm^2) or transmission of $\approx 10^{-6}$ for several threshold detectors.

Figure 15 shows a general view of the shielding

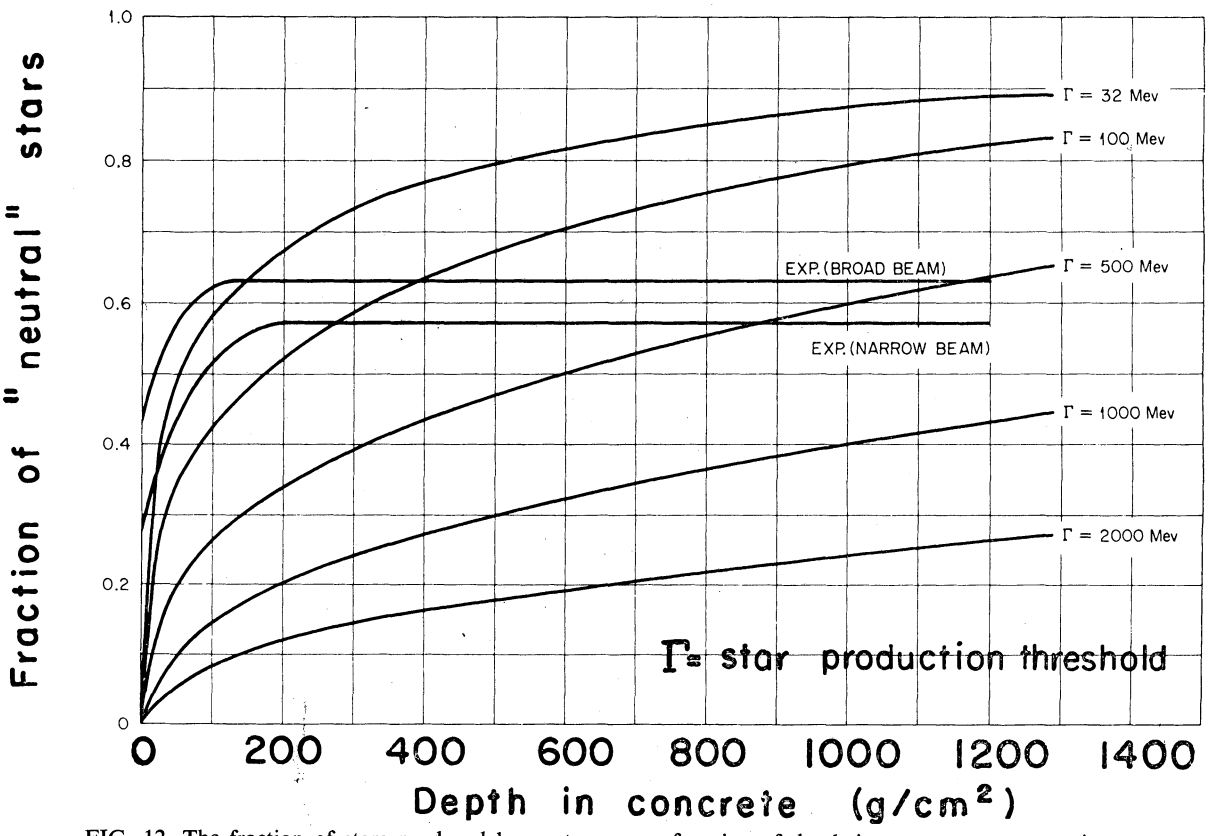

FIG. 12. The fraction of stars produced by neutrons as a function of depth in concrete—a comparison between experimental and calculated data. Incident proton energy 24 GeV. (After Alsmiller and Murphy.)

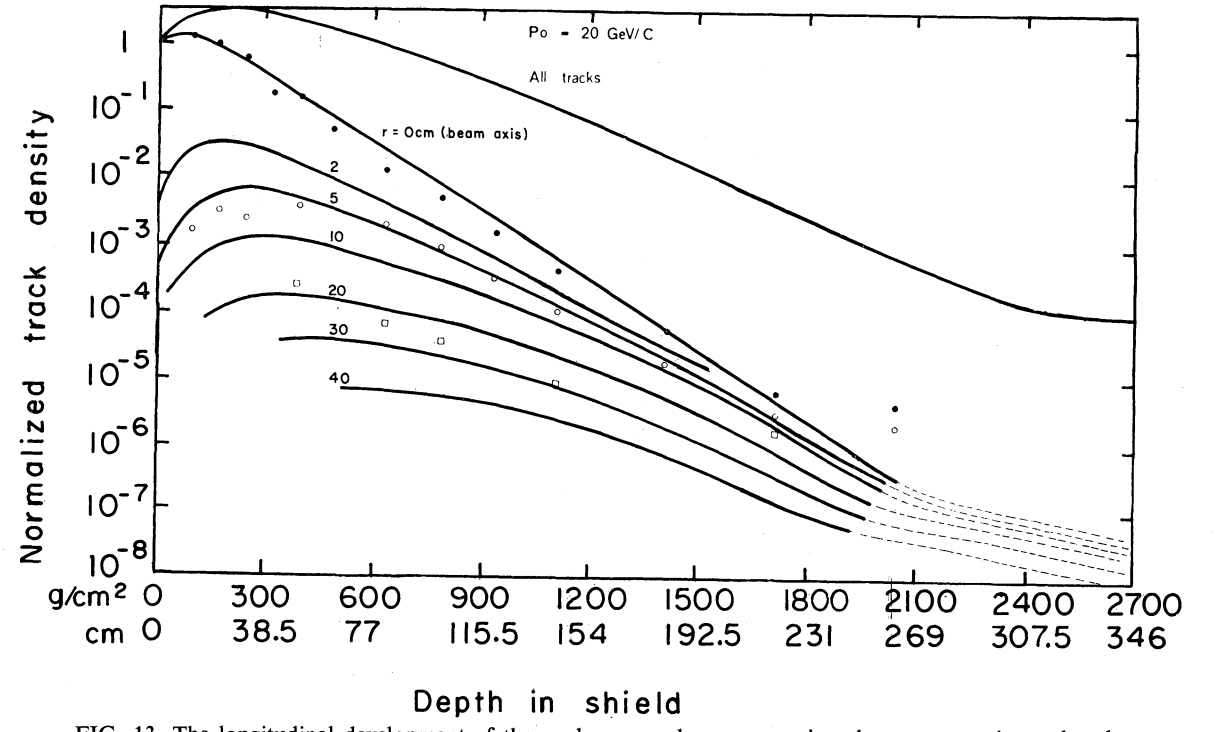

FIG. 13. The longitudinal development of the nuclear cascade—a comparison between experimental and calculated data. The curves show the calculated total track density (sum of proton, pion, and muon track densities) for a cascade initiated by a well-collimated proton beam of cross section 1×1 cm and initial momentum 20 GeV/c. The curves are normalized to unit proton track density at $r = 0$, $Z = 0$. The points represent the measured track densities along the beam axis ($r = 0$) (●) and 8 (○) and 32 cm (□) distant from the axis ($r = 8$, 32 cm) by Citron *et al.* (Ref. 53). The change in slope of the curves near a depth of $z = 2000$ g/cm² arises from the muon track density. (After Ranft.)

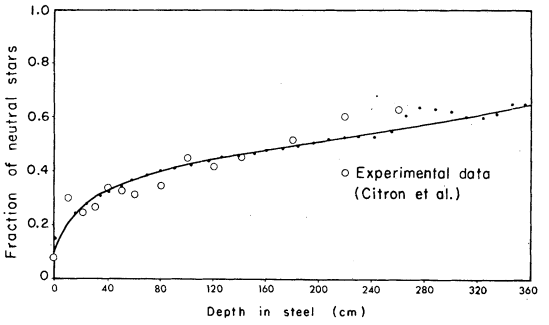

FIG. 14. Fraction of neutral stars as a function of depth in steel—comparison between calculated and measured values. Incident proton momentum 20 GeV/c. (After Ranft.)

array and gives an impression of the size of the structure, which was designed to be large enough to prevent interference from stray radiation scattered in from the sides. The assembly consisted of ordinary concrete in block form, and was 28 ft thick along the beam direction, 22 ft wide, and 18 ft high. Several special thin blocks were placed at the front of the array (not visible in Fig. 15); deeper in the stack, slots provide access to the beam line at intervals of 4 feet. Rows of blocks were separated by 3-in.-wide gaps to allow insertion of detectors, but all portions of these gaps are filled with gypsum (approximately same density as concrete) to prevent neutron diffusion along the slots.

Two principal goals were set for the experiment. The first was to extend the information obtained at CERN to neutrons of much lower energy. This was achieved by the use of various activation detectors with thresholds between 3 and 20 MeV. Secondly, the experiment was designed to test in a

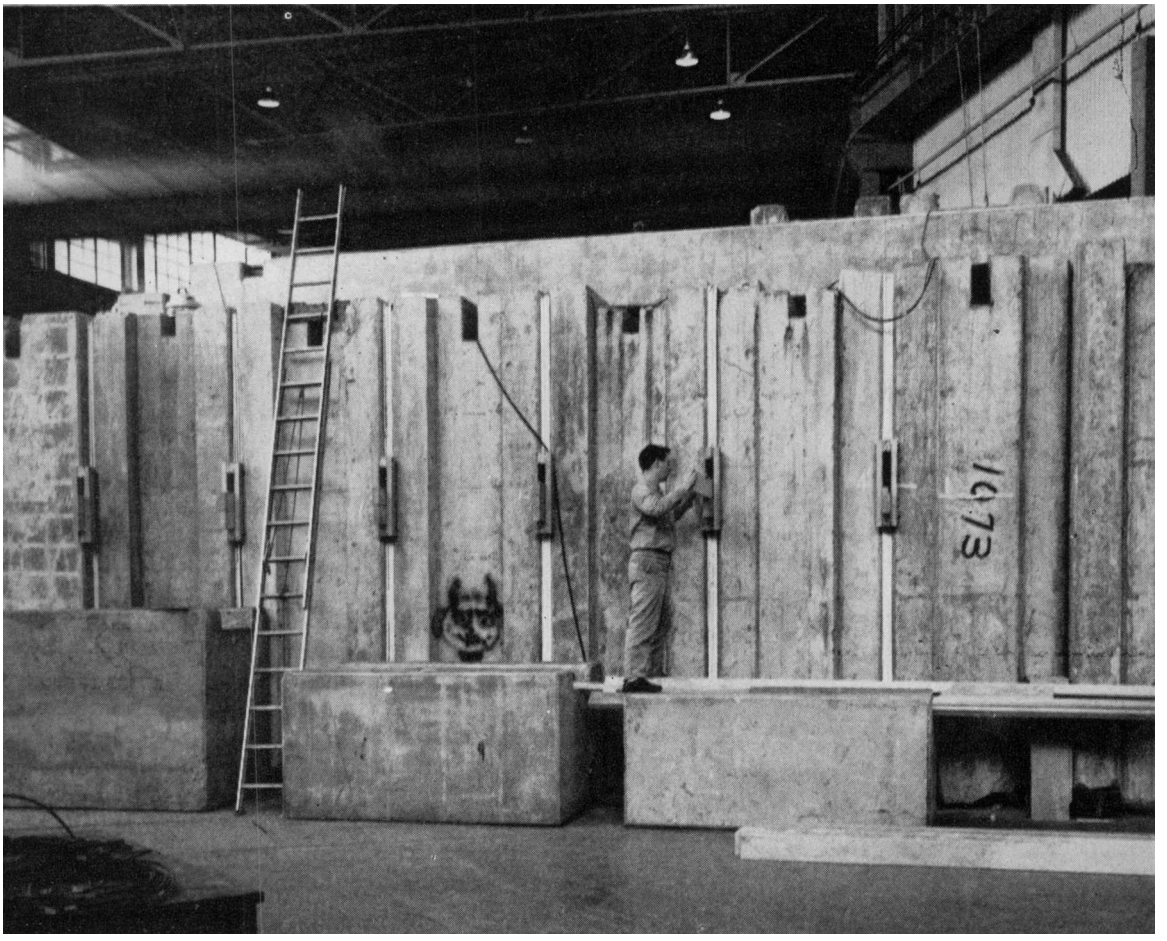

FIG. 15. Shielding experiment at the Bevatron. The proton beam is incident from the left. Radiation detectors are being placed in position.

systematic way some of the predictions of the 'Moyer Model.' It will be recalled that this phenomenological model had met with some success in extrapolating shielding for the Bevatron and that it might usefully be generalized. Since the Moyer model posits that the transmission of the nuclear cascade is controlled by high-energy neutrons and that an equilibrium cascade is rapidly created, measurements of low-energy neutrons form a sensitive test of the model.

Details of the experimental data obtained have been given by Smith, McCaslin, and Pick[61] and Smith,[47] who described data obtained with activation detectors, and by Thomas,[62] who described data obtained by using nuclear emulsions and measurements of the activity induced in sulfur measured by Shaw[63] of the Rutherford Laboratory.

Figure 16 shows typical lateral flux-density profiles measured in the assembly—in this case by using the 6-MeV threshold reaction $^{27}Al(n, \alpha)^{24}Na$. Similar data were obtained for thermal neutrons and by using the $^{32}S(n, p)^{32}P$ and $^{12}C(^{n, 2n}_{p, pn})^{11}C$ reactions. From such traverses, the transmission of flux density from the front of the shield assembly, at a given angle to beam direction, was obtained.

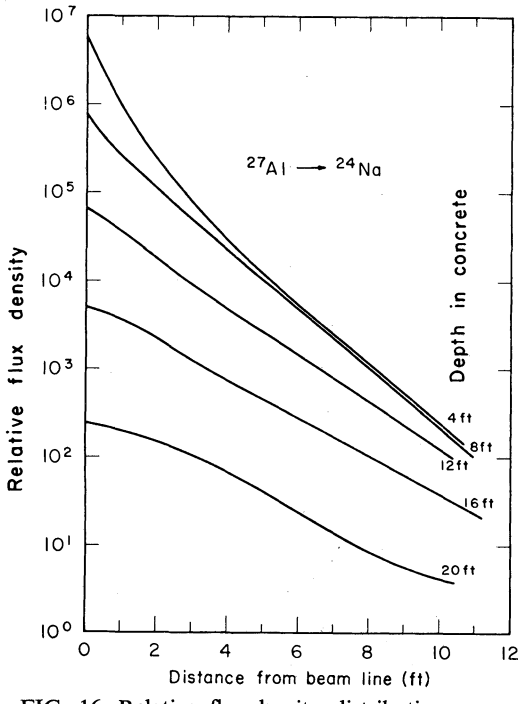

FIG. 16. Relative flux-density distributions normal to the incident beam direction measured in concrete by using the ($^{27}Al \rightarrow {}^{24}Na$) reaction. Incident proton energy 6 GeV. (After Smith *et al.*)

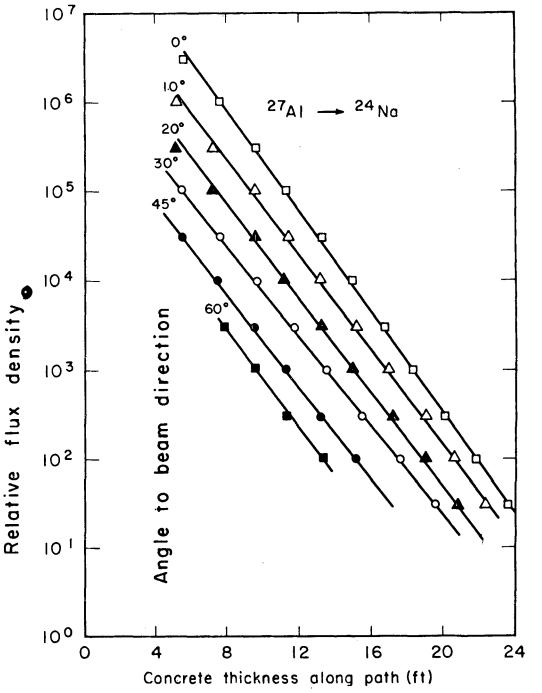

FIG. 17. Relative flux-density distribution measurements along paths drawn at several angles to the point of incidence of the proton beam on the concrete shield. Measurements made with the $^{27}Al \rightarrow {}^{24}Na$ reaction. Incident proton energy 6 GeV. (After Smith *et al.*)

Figure 17 shows such data for the *Al* activation detector for angles up to 60 deg. These transmission curves are seen to be exponential and essentially parallel within the experimental accuracy. (The errors were *no larger* than point size indicated.) Similar results were obtained with ^{12}C threshold detectors.

Figure 18 shows transmission measurements along the beam direction made with gold, aluminum, and carbon detectors. A steady progression in slopes of the transmission curves is evident—the slopes tend to become similar at great depths but the curves are not identical. The data have been normalized at a depth of 8 ft in the assembly to show this effect clearly. At great depths the carbon detector gives an effective attenuation length of 108 g/cm^2; the *Al* and *Au* detectors give 114 and 120 g/cm^2, respectively. Smith interprets this result as evidence that complete equilibrium is not established until rather deep depths in the concrete are reached—say, 12 to 16 ft. In support of this view Fig. 19 shows that the ratio of activity measured by carbon and aluminum detectors

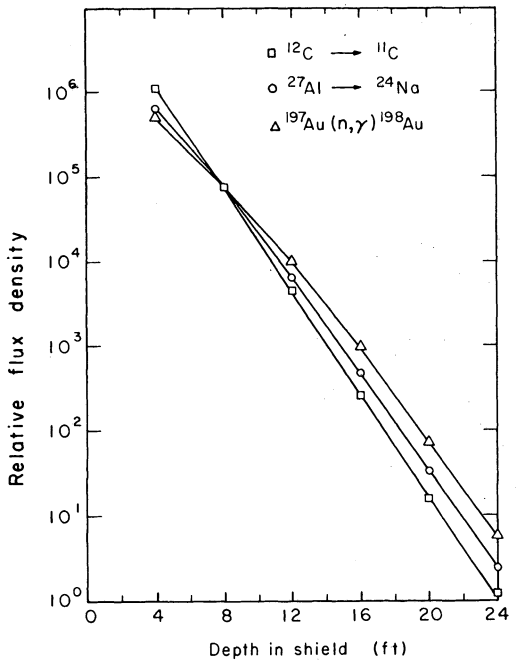

FIG. 18. Relative flux density along beam axis. Measurements made with $^{197}Au(n,\gamma)^{198}Au$, $^{27}Al \rightarrow {}^{24}Na$, and $^{12}C \rightarrow {}^{11}C$ reactions. Data normalized at a depth of 8 ft in concrete. Incident proton energy 6 GeV. (After Smith *et al.*)

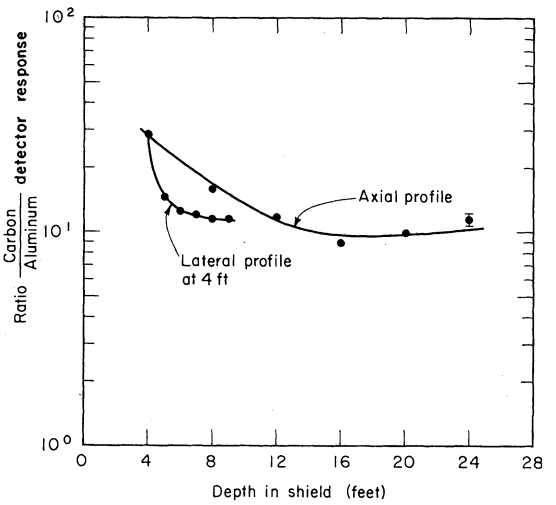

FIG. 19. Typical example of the ratio of detector response as a function of distance from the point of incidence to the proton beam on the shield. The curve labeled 'axial profile' was obtained in the beam direction; that labeled 'lateral profile' was obtained at a depth of 4 ft into the shield in a direction normal to the beam direction. Incident proton energy 6 GeV. (After Smith.)

becomes constant at deep depths in the beam direction. In the transverse direction, however, equilibrium is more rapidly attained. In further support of his hypothesis that equilibrium is not reached at shallow depths, Smith reports measurements made with the same detector but with varying initial proton energy—between 2.2 and 6.2 GeV. The lower the primary beam energy, the lower the apparent attenuation length, values ranging from 99 to 114 g/cm² being obtained (see Fig. 20).

Unfortunately the experimental data obtained in this experiment were not numerically analyzed by a technique similar to that described by Gilbert *et al.*[44] The successful use of the Moyer model in interpreting the latter experiment may now encourage this step. It is clear, however, that the data give strong support for the basic premises of the Moyer model, namely:

1. the transmission of particle fluxes with an attenuation length independent of angle to the radiation source,
2. the establishment of an equilibrium spectrum at sufficiently deep depths in the shield.

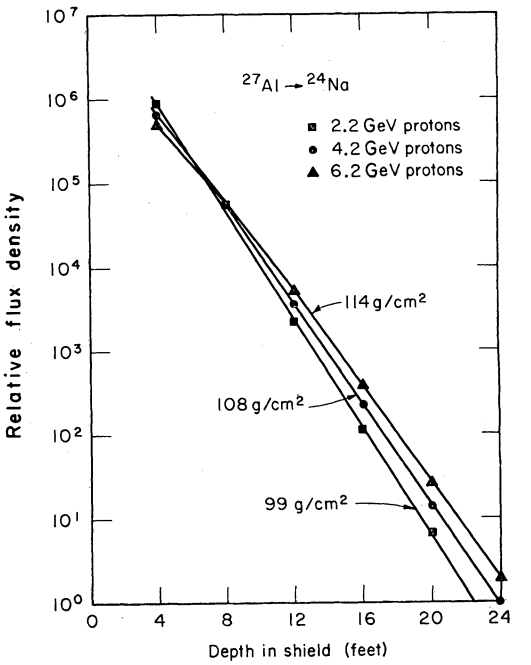

FIG. 20. Flux-density transmission along the beam axis measured by aluminum threshold detectors for protons of 2.2, 4.2, and 6.2 GeV. (After Smith.)

5. BROOKHAVEN AGS EXPERIMENT

Significant as the CERN and Berkeley experiments were in the development of our understanding of the nuclear cascade, they left many questions unanswered. They were primarily concerned with the development of the nuclear cascade in the forward direction; but in the design of the permanent shielding of a large high-energy accelerator, knowledge of the transverse development of the nuclear cascade is also needed as well as the spectrum of radiation field produced.

In planning for an increase in intensity of the Brookhaven AGS measurements of particle attenuation transverse to the beam in both the accelerator room and the shield were made. Circulating 30-GeV protons struck an internal Be target, and radiation measurements were made by activation detectors and photographic film. In the accelerator room, flux densities were measured around the beam axis downstream from the target, giving the isoflux contours shown in Fig. 21. The approximately cylindrical nature of these contours[64] led Moore[65] to interpret the flux density from the target by the equation

$$\phi(r, \theta) = \frac{k}{r^2\theta^2} \; 20 \text{ deg} \leqslant \theta \leqslant 90 \text{ deg}, \qquad (10)$$

where $\phi(r, \theta)$ is the flux density of particles greater than 20 MeV,

r is the distance from the target,
and θ is the angle from the beam direction.

With r measured in feet and θ in degrees, Moore found a value of k of 1.5 per circulating 30-GeV proton. In commenting upon the $1/\theta^2$ from the angular distribution Moore drew attention to the similar result reported by Hoffman and Sullivan[66] measured around a thin beryllium target. More recent angular distribution measurements by Charlambus *et al.*[67] at 20 GeV and by Gilbert *et al.*[44] at 15 and 25 GeV show the suggested $1/\theta^2$ form to be a fair approximation. From Eq. (10) Moore deduces that 24 particles having energy greater than 20 MeV are produced per 30-GeV proton incident upon a Be target.

To study the transmission of radiation through the AGS shielding, vertical holes were drilled through the sand above accelerator magnets and in the side shielding. These holes allowed measurements to be made through 10 feet of sand vertically above the accelerator and through 20 feet of sand to the side.

Typical transmission data obtained vertically above the accelerator are shown in Fig. 22.[67] Over the limited range possible (≈ 50 in attenuation) the relaxation length of flux density was evaluated to be 83 g/cm^2. To extend data to greater depth, measurements were made in the median plane, and typical results are shown in Fig. 23. The strong influence of geometrical factors on the data is clearly seen, making a simple interpretation difficult. Casey *et al.*[68] summarize their results by an exponential transmission of flux density (or dose rate) with relaxation length

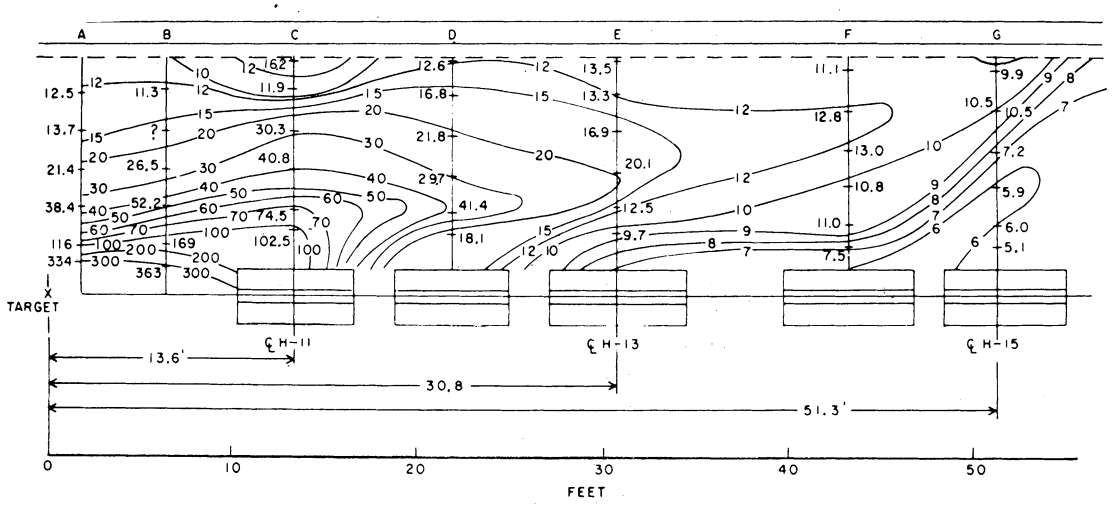

FIG. 21. Flux-density distribution in the AGS accelerator tunnel around an internal target. Measurements made with polyethylene foils and 2.78×10^{11} protons incident upon a thin Be target. The relative accuracy of contours is ≈ 10 per cent. (After Casey *et al.*)

83 g/cm² (using a measured value of 1.82 g/cm³ for the density of earth). They suggest, however, that the exponential character is fortuitous, resulting from a special combination of geometry, angular distribution of secondaries from the target, and change in interaction length at various inclinations to the beam direction.

O'Brien and McLaughlin[69] have applied polynomial neutron transport theory[70] to neutrons of 500 MeV and below, generated in a nuclear cascade, and compared their calculations with measurements reported by Distenfeld and Colvett.[71] Figure 24 shows a comparison between calculated and measured attenuation of neutrons having an energy greater than 20 MeV. Agreement between the normalized data is seen to be good.

Although these techniques have been successful in describing relative neutron transmission through accelerator shields, it has not yet been possible to make an *absolute* comparison of theoretically predicted and measured neutron flux densities. Recent calculations of neutron dose-equivalent rates from galactic cosmic rays by such techniques has revealed only fair agreement with measured values, however.[72]

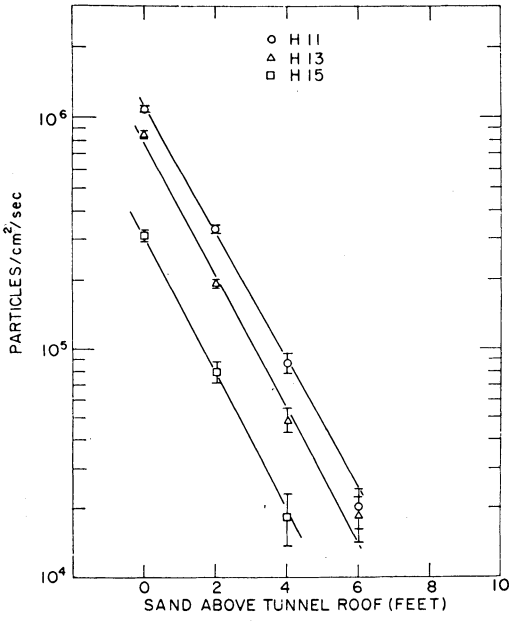

FIG. 22. Variation of flux density in sand shield of the AGS. Measurement with carbon activation detectors. Beam intensity 2.8×10^{11} protons/sec on target in straight section H10. Measurements made in vertical direction at mid-magnet positions H11, H13, and H15. (After Casey *et al.*)

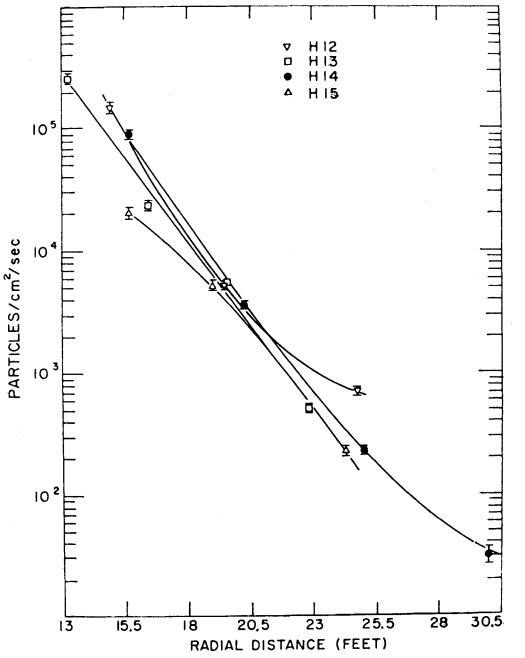

FIG. 23. Variation of flux density in sand shield of the AGS—horizontal direction. Other conditions as for Fig. 22. Measurements made at mid-magnet positions H12, H13, H14, H15. (After Casey *et al.*)

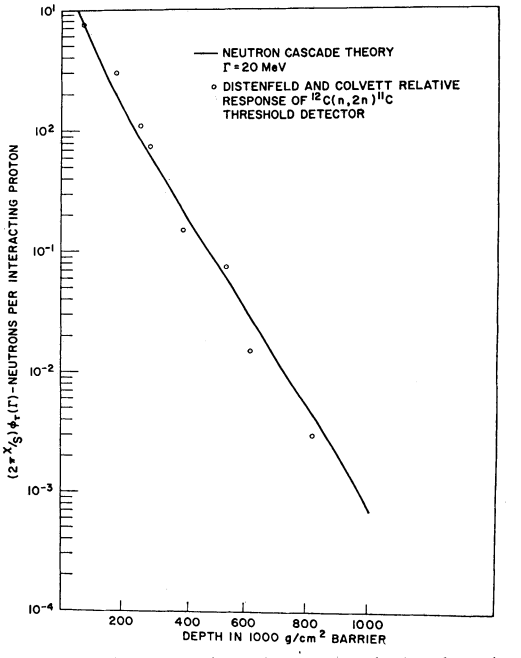

FIG. 24. A comparison between calculated and measured relative neutron transmission through the sand shield of the Brookhaven AGS. (After O'Brien and McLaughlin.)

Casey *et al.* concluded that particle attenuation transverse to the beam direction was much more rapid than would be concluded from calculations based on strongly interacting particle interaction lengths. This suggestion is in conflict with the Moyer model, and of such interest as to stimulate further studies.

6. CERN-LRL-RHEL SHIELDING EXPERIMENT

Following the work at Brookhaven, another experiment was planned at the CERN PS by groups drawn from CERN, the Lawrence Radiation Laboratory—Berkeley, and the Rutherford Laboratory, all of whom were actively engaged in the design of accelerators in the several-hundred-GeV range. The goals of this experiment, designed to answer many of the questions posed by the Brookhaven measurements, were:

1. Study of the transmission of particles through earth shielding, principally at 90 deg to an internal target in the accelerator.
2. Measurement of neutron spectra at different depths in the earth shield.
3. Measurement of the angular distribution of high energy particles from an internal target.

As at the AGS, vertical holes were drilled in the earth shield above and to the side of the accelerator. Figure 25 shows a vertical cross section of the CPS tunnel, indicating hole locations; Fig. 26 shows a plan view of the area in which radiation measurements were made in the shielding.

Extensive discussions of the experimental data obtained have been published,[44, 73–76] and it is possible to give only a brief discussion here.

Figure 27 shows some details of actual measurements of beam losses made with aluminum foils on the accelerator vacuum chamber close to an internal target. Fine structure due to the presence of accelerator magnets may be seen. Subsequent analysis of these data showed the beam-loss distribution about the target to be represented sufficiently accurately by a base level, α, representing the average low-level losses with a target contribution superposed which decreased in intensity downstream from the target. Thus the beam loss $s(z)$ may be represented by the equations:

$$s(z) = \alpha \qquad z < 0, \qquad (11a)$$

$$s(z) = \alpha(1 + \beta e^{-z/\mu}) \qquad z > 0, \qquad (11b)$$

where z is measured from the target position.

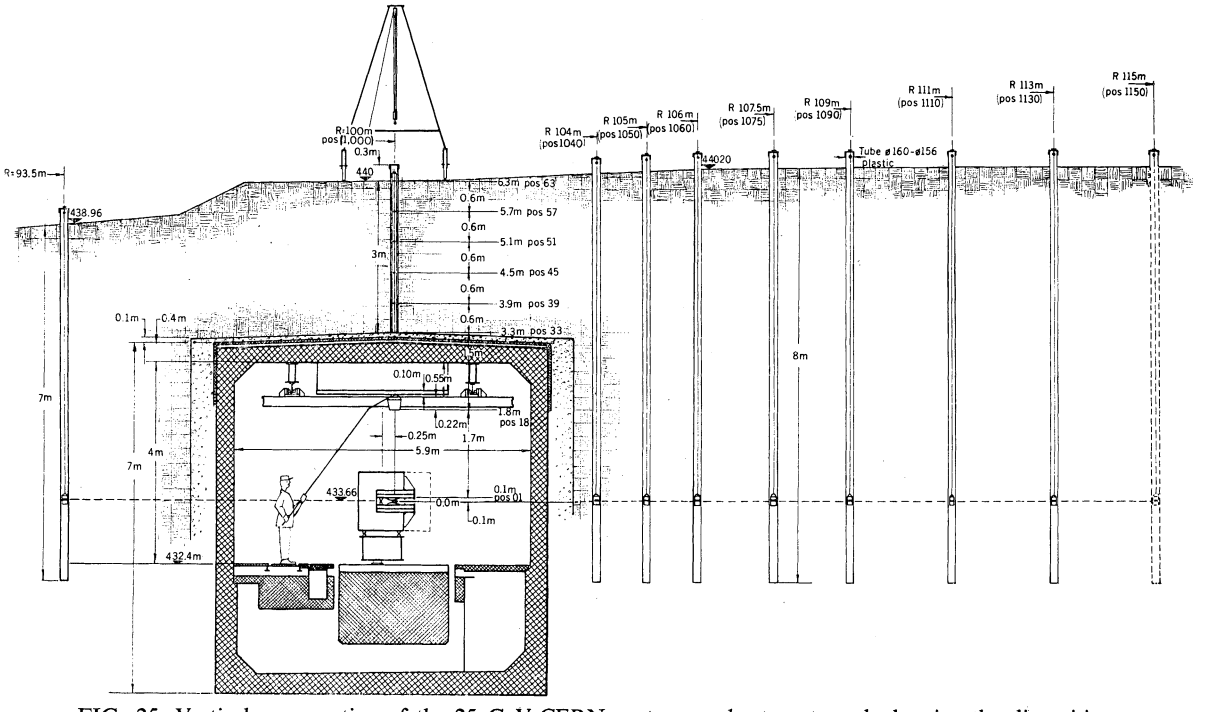

FIG. 25. Vertical cross section of the 25-GeV CERN proton synchrotron tunnel, showing the disposition of detector holes in the earth shield. (After Gilbert *et al.*)

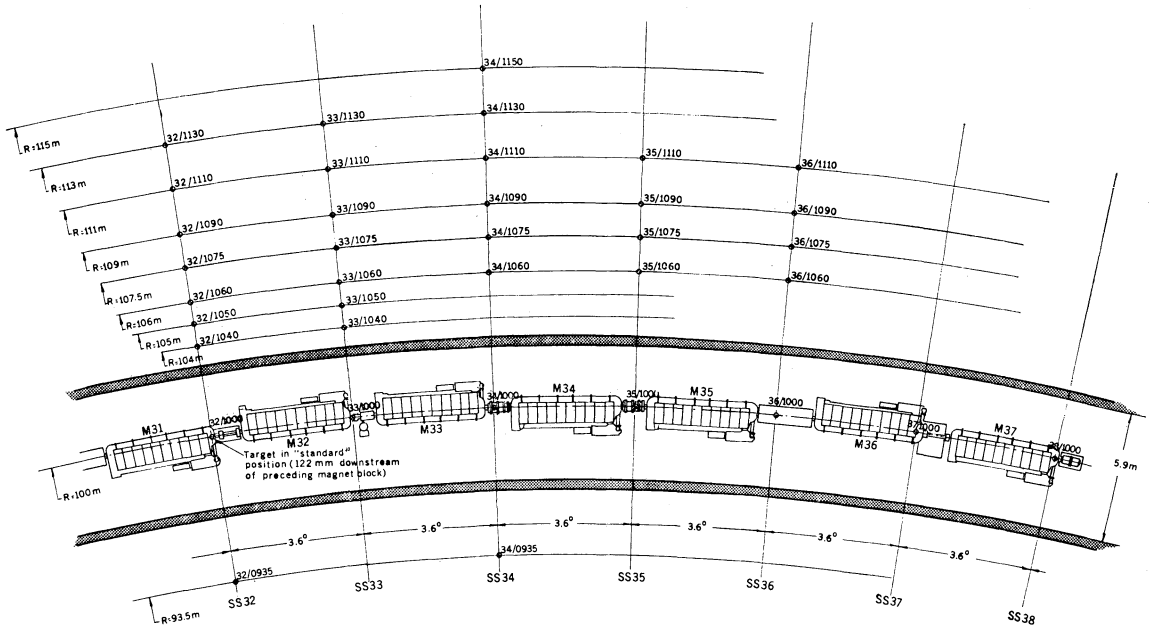

FIG. 26. Plan view of the CPS, showing the disposition of detector holes in the earth shield. (After Gilbert *et al.*)

More sophisticated analytical representation of the data,[77, 78] or even use of the actual numerical data, does not produce any significant improvement in the quality of fit to measured fluxes in the earth shield,[44] and it may therefore be inferred that Eq. (11) is an adequate representation of the source term for the CPS. It might quite correctly be objected that the relative activities of aluminum foils which are sensitive to rather low-energy particles only indirectly reflect the high-energy proton source structure. It would have been preferable to use detectors with a much higher energy threshold, but this was technically not feasible at the time measurements were made. However, measurements with other low-energy detectors gave the same results and support the view that no serious error is involved, as also do Monte Carlo estimates of beam loss by Ranft[79] (Fig. 28). At large distances from internal targets such a simple prescription as Eq. (11) fails at the CPS, the beam loss at levels ≈ 1 per cent of the maximum being somewhat random.[44] The approximately exponential reduction of target contribution to the beam losses with distance from the target that was observed at the CPS will not necessarily be observed at other accelerators. A somewhat different distribution was observed, for example, at the

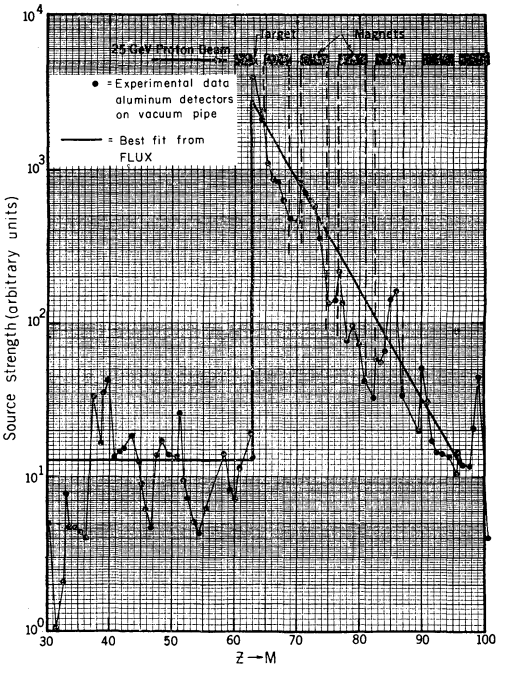

FIG. 27. Fine-structure details of the beam-loss distribution measured in the vacuum chamber of the CPS close to an internal target. (After Gilbert *et al.*)

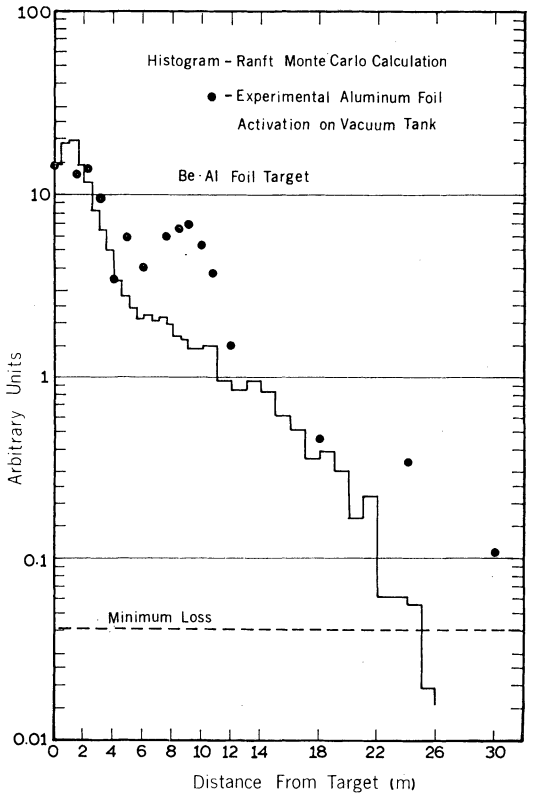

FIG. 28. Comparison of measured beam-loss distribution with Monte Carlo calculations due to Ranft. (After Gilbert *et al.*)

AGS.[68] The precise details of the beam-loss distribution is of course a complex function of target dimensions, magnet spacing, and physical size, accelerator magnetic field configuration, and other accelerator characteristics. It is nevertheless important to have good estimates of the beam-loss distribution pattern if the distribution of secondary particles through the shield is to be understood. Awschalom[78] has indicated that large errors (as much as a factor of 10) can result in estimates of flux densities if no account is taken of source distribution.

It is important to understand not only spatial distribution of beam losses but also the angular distribution of neutrons emitted from the primary beam interactions.

Figures 29 and 30 show measurements of the angular distribution of neutrons from a thin Be target made with activation detectors having thresholds of 20 and 600 MeV respectively. A comparison with the angular distribution predicted by Ranft[80] is surprisingly good, giving confidence in Ranft's semi-empirical formula. Routti and Thomas[81] have used Ranft's formula to calculate the angular distribution of protons greater than 150 MeV from a thin Be target and shown that the *shape* of the distribution about 90 deg is nearly independent of primary proton energy between 1 and 300 GeV. For angles around 90 deg., the angular distribution may be expressed[45] by a simple exponential form,

$$\Theta(\theta) = \gamma e^{-\eta\theta}. \tag{12}$$

Figure 31 shows the angular distribution of neutrons greater than 150 MeV produced by 14-GeV protons incident upon beryllium and iron targets compared with the function $\exp(-4\theta)$. Routti and Thomas[45] conclude such an angular distribution should be used in the estimation of transverse shielding when Eq. (7) is used.

Preliminary results of the CERN shielding experiment reported by Gilbert *et al.* indicated that a simple exponential model of transmission was inadequate, because the attenuation length inferred is a function of the assumed geometry, and also of position relative to the target at which the measurement was made. Figure 32 shows the result of

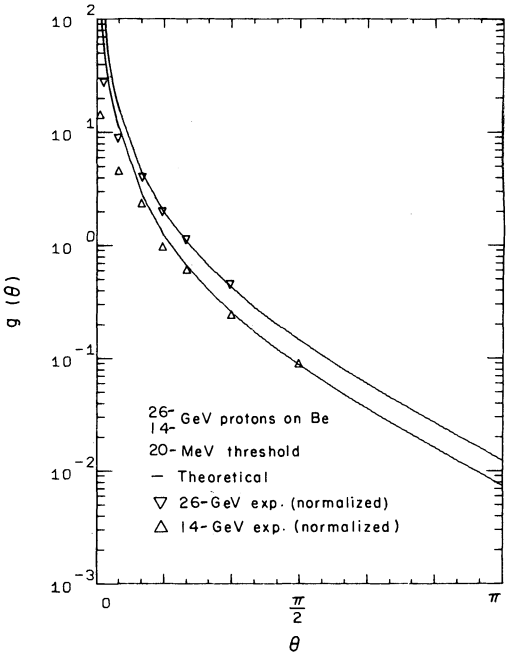

FIG. 29. The angular distribution of neutrons above 20 MeV energy produced by 26- and 14-GeV proton beam incident on a thin target, as measured by Gilbert *et al.*, and calculated from Ranft's semi-empirical formula. (After Routti and Thomas.)

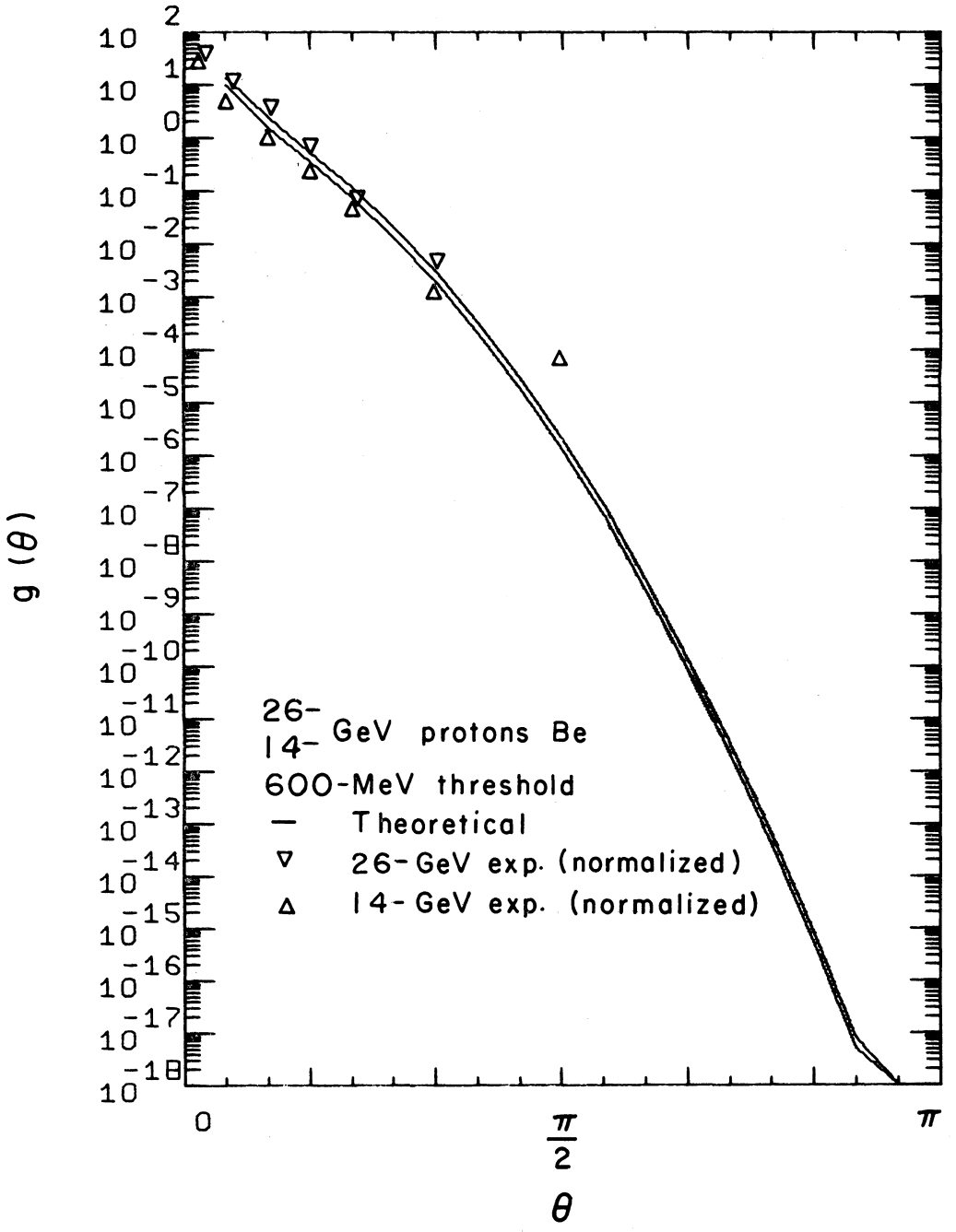

FIG. 30. The angular distribution of neutrons above 600 MeV energy produced by 26- and 14-GeV proton beam incident on a thin target, as measured by Gilbert *et al.*, and calculated from Ranft's semi-empirical formula. (After Routti and Thomas.)

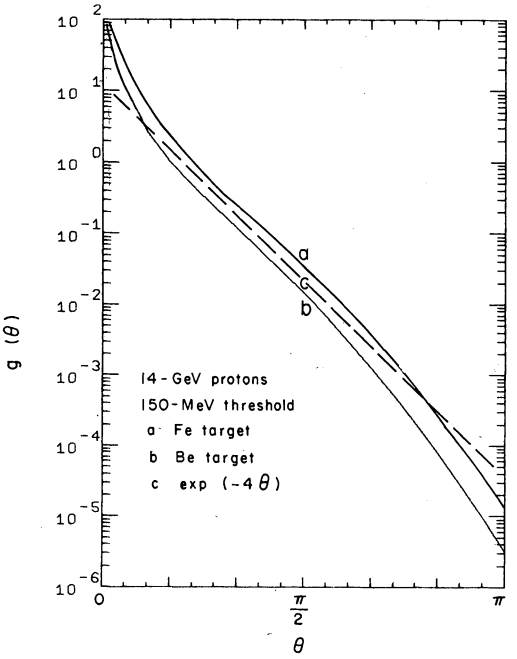

FIG. 31. The angular distribution of neutrons above 150 MeV energy produced by 14–GeV protons incident on thin Fe and Be targets, as calculated from Ranft's semi-empirical formula. (After Routti and Thomas.)

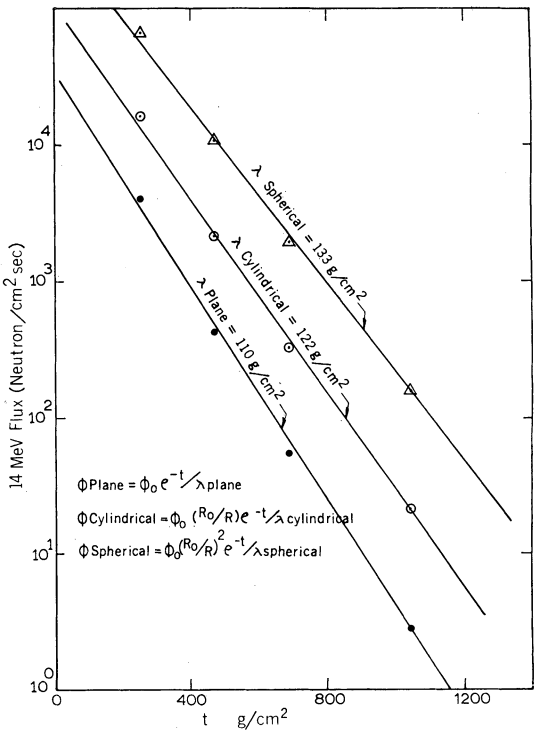

FIG. 32. The influence of geometrical models on apparent attenuation length. (After Gilbert *et al.*)

expressing identical flux measurements in terms of different geometrical models. Although of high accuracy ($\approx$ 3 per cent), the data are nevertheless inadequate of themselves to permit any objective choice as to the preferred geometrical model. Additional information is therefore required if the relaxation lengths obtained from shielding experiments are to be related to particle attenuation lengths. The influence of source distribution on relaxation length is indicated in Fig. 33, which shows the vertical attenuation of neutron flux as measured with aluminum activation detectors in three locations. Although the experimental data are well fitted by straight lines (exponentials), it is incorrect to assume, without incorporating geometrical effects and the influence of source shape, that the slopes of these lines yield the attenuation mean free path in earth.

Because the CERN experimental data in the earth shield were so extensive, analysis was attempted in terms of the simple phenomenological model first derived by Moyer. The flux at a point in the shield was written as

$$\phi_p = \int S(z)\, \Theta(\theta) e^{-x/\lambda}\, d\Omega\, dz \qquad (13)$$

where $S(z)$ is the number of protons interacting in a line element dz,
$\Theta(\theta)$ is the angular distribution of particles at the target,
x is the total shield thickness traversed,
λ is the attenuation length.

The practical problem of analysis consisted of two parts—the first of defining realistic physical functions for $S(z)$ and $\Theta(\theta)$ (appropriate functional forms have already been discussed), and the second of obtaining the 'best fit values' for the parameters of the functions.

A computer program—FLUXFT—developed by Close,[82] incorporates an appropriate geometry subroutine and a minimization procedure that may operate with up to eight parameters. It was used to analyze the data and to describe experimental flux measurements ranging over distances of nearly 100 meters from the target and over a flux range of $\approx 10^5$ by only five independent parameters (mean free path, angular distribution coefficient, source relaxation length, and two normalization constants). Typical results (Fig. 34) showed that the single set of parameters could fit measured data to an average accuracy to within less than 20 per cent

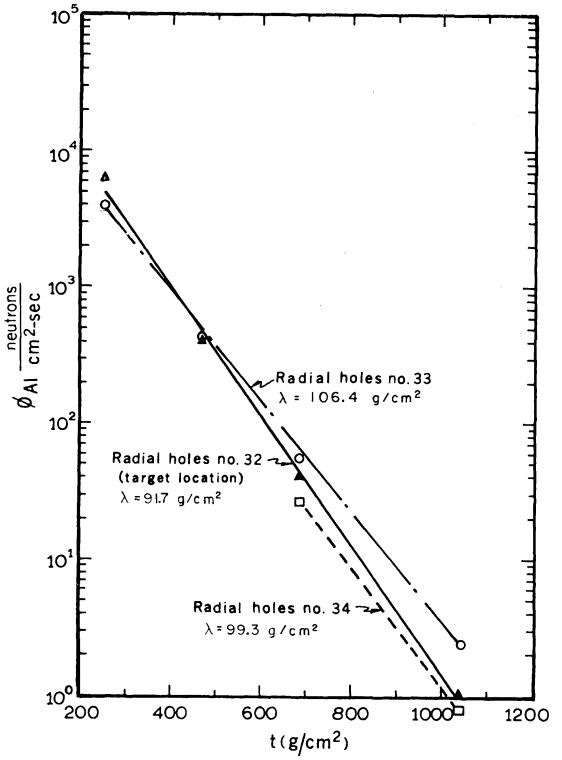

FIG. 33. The influence of source distribution on relaxation length.

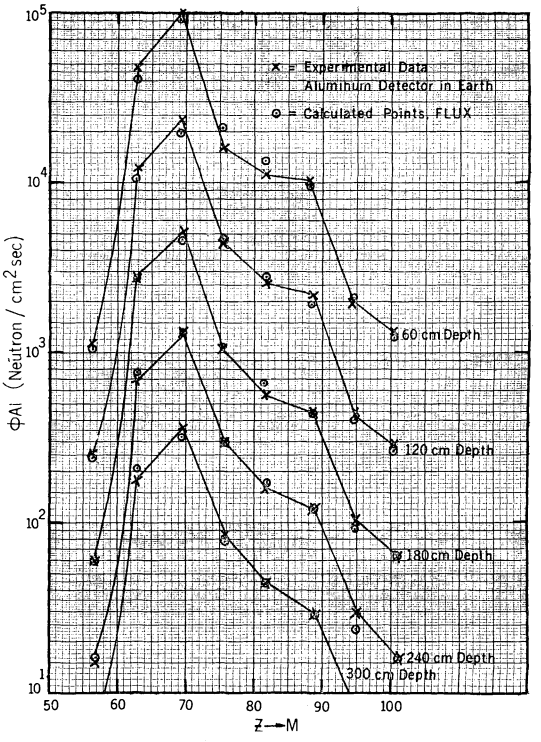

FIG. 34. Examples of typical fits to experimental data obtained at CERN when FLUXFT is used. (After Gilbert *et al.*)

over an attenuation range of 10^5. As might be expected, the attenuation length in earth was quite well constrained to 117 ± 2 g/cm². The angular distribution coefficient, η, is not so well constrained, but has a value between 2 and 2.5 for flux densities of energy greater than 20 MeV. The quality of the fit finally obtained by using these best-fit parameters is indicative of the excellence of the phenomenological model.

Routti and Thomas[45] have used the experimental data obtained at CERN to derive a simple expression for the shield thickness required for an accelerator with uniform beam loss in the geometry shown in Fig. 3. They write

$$DE = \frac{L}{(a+\mathrm{d})} M(4, \mathrm{d}/\lambda), \tag{14}$$

where DE is dose-equivalent rate, in mrem/h at the shield surface,

L is uniform beam loss rate, in GeV/cm sec,

λ is attenuation length of high-energy neutrons, and

a, d are explained in Fig. 3 and measured in meters.

The Moyer Integral[45] $M(4, \mathrm{d}/\lambda)$ is given by

$$M(4, \mathrm{d}/\lambda) = \int_0^{\pi} \exp(-4\theta) \exp\left(\frac{-\mathrm{d}\ \mathrm{cosec}\ \theta}{\lambda}\right) \mathrm{d}\,\theta. \tag{15}$$

A comparison between shield estimates made for 200-GeV and 300-GeV accelerators, using Eq. (15) and extrapolation of the experimental data reported by Gilbert *et al.*,[44] is given in Table V. The agreement is seen to be good.

Values of Moyer Integrals have been tabulated,[45] and using the values

$$\lambda = 53.9 \text{ cm} = 116.5 \text{ g/cm}^2,$$

$$a = 2.8 \text{ m},$$

Routti and Thomas obtain for the required total shielding thickness, t, as a function of L/D, the simple expression

$$t(\mathrm{g/cm^2}) = 230 \log_{10}\left(\frac{L\ [\mathrm{GeV/cm\ sec}]}{D\ [\mathrm{mrem/h}]}\right) - 610. \tag{16}$$

This simple formula, however, applies only to regions of fairly uniform beam loss.

TABLE V

Calculated shield thicknesses for high energy proton synchrotrons.

Accelerator	Energy (GeV)	Beam loss (p/sec)	Radius (m)	(GeV per cm sec)	D (mrem/h)	L/D	Total shield thickness including magnet (g/cm²) Magnet thickness (g/cm²)	Gilbert et al. (Ref. 44)	Routti & Thomas (Ref. 45)
CPS	25.5	2×10^{11}	100	1.8×10^{7}	0.8[a]	2.3×10^{7}[b]	400	1085[c]	1085[c]
CPS	25.5	10^{12}	100	9.0×10^{7}	0.8	1.1×10^{8}[b]	400	1240	1240
CPS	25.5	10^{13}	100	9.0×10^{8}	0.8	1.1×10^{9}[b]	400	1455	1470
LRL design study (Ref. 19)	200.	2×10^{12}	693	9.2×10^{8}	1.25	7.4×10^{8}	280	1440	1430
CERN design study (Ref. 20)	200.	2×10^{12}	693	9.2×10^{8}	0.25	3.7×10^{9}	280	1600	1590
	300.	6×10^{12}	1200	2.4×10^{9}	0.8	3.0×10^{9}	300	1585	1570

a. Experimental value (Ref. 44).
b. Effective value due to beam clipper (Ref. 44).
c. Normalized to the same value.

Above the internal targets the use of this simple formula is not very precise. Typically the value of L/D above the targets is some two orders of magnitude higher than in the regions of low beam loss. Such as assumption with the Moyer Integrals leads to a conservative estimate. For precise shield configurations detailed beam-loss distribution should be used.

In summary, the use of the Moyer Integrals allows rapid and accurate estimates of the high-energy neutron flux above different threshold energies as well as the dose-equivalent rate to be found at the surface of proton accelerator shields operating in the energy region 5 to 500 GeV.

The precision for the flux and dose-rate estimates in regions of uniform beam loss is likely to be better than a factor of 2, and even in target regions the dose-rate estimates are fairly reliable.

7. SUMMARY AND A LOOK INTO THE FUTURE

We have seen that radiation studies made during the 1960's at high-energy accelerators confirmed the intuition of Moyer and Lindenbaum. The early (1960–63) CERN experiments distinguished between attenuation on beam axis and 'lateral integrated' attenuation, but did not completely succeed in identifying the attenuation length appropriate to accelerator shield design. Nuclear emulsions proved to be an invaluable visual technique facilitating a description of the cascade development. In 1964 the development of extracted proton beams at the Bevatron facilitated studies of the low-energy neutrons produced in the cascade and the first attempts at neutron spectrum measurement. As yet no formal analysis of these straight-ahead shielding measurements has been attempted in terms of a phenomenological model such as that due to Moyer, although both series of experiments can be interpreted to confirm its basic assumption. Measurements at great depths in the shield at Berkeley indicated the presence of an equilibrium spectrum at low energies and much lower attenuation lengths than had previously been reported—close to that predicted by use of high-energy inelastic cross sections.

As the very large 200- to 500-GeV proton accelerators were designed, the emphasis and interest shifted from straight-ahead to transverse shielding, because such shielding is a substantial capital investment for such large machines. At present interest has reverted to straight-ahead experiments because of the need to design adequate beam backstops for disposal of the intense beams extracted from the strong-focusing synchrotrons. Thus Levine and Moore[83, 84] have reported studies in a composite assembly of tungsten, uranium, steel, and concrete. Both the strongly interacting flux densities in the stack and the mean

flux density emerging from the assembly were measured. Although preliminary, the measurements are of interest in that they are the first attempts to study the influence of a magnetic field on the dispersion of the muons. Goebel and Ranft[85] have reported a comparison between neutron flux densities of energy greater than 100 MeV calculated by Monte Carlo techniques and measurements with threshold detectors outside a 3-meter-long beam stop. Agreement was obtained in general within a factor of 2.

The advances in our understanding of the development and transmission of the nuclear cascade in matter summarized here have made it possible to design accelerator shields with fair precision. This will facilitate economies in the shielding construction, and it is self-evident in these difficult financial times that every effort will be made by designers to reduce the investment in static blocks of steel and concrete! This is of course to be lauded and encouraged, but some words of caution are needed. All is not yet perfect in our understanding, and it would be ironic if the mistakes of the fifties were repeated in the seventies in a display of overconfidence. To check the accuracy of existing calculational models it would be desirable to plan future, 'shielding measurements' so that the experimental results obtained are in a form susceptible of calculation. Conversely, theoreticians might be persuaded to make calculations in terms of the radiation detectors available to the experimenter, and in realistic shielding materials. In the opinion of the authors, the Berkeley-CERN-Rutherford shielding experiment represents an experiment capable of testing theoretical calculations with some severity. The density and composition of the shield is known with some accuracy; flux-density measurements were made with a variety of threshold detectors; the primary proton-loss pattern is well known; and so is the geometry of the experiment. Although calculations in an actual, rather than simulated, shield for the complex geometry involved may be tedious, such a comparison is ultimately necessary to test cascade models. The increasing capability of Monte Carlo calculations and other computational techniques is encouraging—it might eventually be possible to simulate the precise operational details in the computer and obtain exact estimates of radiation levels. Such calculations, however, are difficult, expensive, and perhaps several years into the future. Furthermore, we must not fall into the trap of leaning too heavily on the results of calculations unsupported by experimental data. The 'proof of the pudding is,' after all, 'in the eating,' and the calculations should stand or fall by their ability to predict observations.

As the accuracy of shielding estimation improves, increasing attention must be given to the location and amount of beam loss. Efforts of heroic proportions are being made at the National Accelerator Laboratory to increase beam-extraction efficiencies to better than 99 per cent,[86] and at Brookhaven studies of beam losses along transported beam are under way.[87] It seems certain that large accelerator operation in the future will combine shields optimized for low beam losses with continuous radiation-monitoring surveillance. High radiation levels, which could result in potential equipment damage or radiation exposure, would then result in rapid shutdown. Slowly increasing radiation levels might well be used to prognosticate imminent component failure and facilitate remedial action before emergency shutdown. Such systems, although demanding less shielding, will require an increasing sophistication in our understanding of radiation fields produced outside accelerator shields.

Thomas[38] has reviewed the studies of the transmission of accelerator-produced radiation at large distances, often referred to as 'Skyshine,' up to mid-1964. He showed that measurements of absolute neutron flux densities at large distances from sources of known intensity were necessary to confirm the predictions by Lindenbaum.[88] Measurements of the relative variation of neutron flux density were, by themselves, of little value in confirming theory unless carried out to very large distances from the radiation source. Distenfeld and Colvett[89] have reported measurements at distances up to 900 metres from the Brookhaven AGS that suggest a somewhat smaller attenuation in air than that suggested by Thomas. The errors on these measurements are, however, rather large, and the influence of other adjacent radiation sources may have been significant. Skyshine has not been a serious problem at high-energy accelerators provided with roof shielding.

The phenomenon known as 'groundshine,' the leakage of radiation underneath heavy-density shielding, was first observed at the Brookhaven AGS around target shielding.[23] Knowles has discussed the problem in the Yale Meson Factory Design Study report,[21] and its solution lies in reducing the scattered radiation by extending the high-density shielding into the lighter-density foundation.[19]

Alsmiller *et al.*[90] have recently made calculations of 'groundshine' for a target bombarded by high-energy protons shielded by iron above an earth foundation. The calculations indicate that close to the shield wall roughly half the observed radiation level is due to groundshine.

Finally, as was indicated by Keefe,[28] muons will represent an increasing problem as the intensity of the 30-GeV accelerators increases, at Serpukhov and at Batavia. Some progress in this area has been reported by the Oak Ridge[91, 92] and NAL[93, 94] groups since the pioneer work of Keefe *et al.*[28, 95–97] but this also remains a major problem for the future.

ACKNOWLEDGEMENTS

The authors wish to thank Dr. William H. Moore (Brookhaven National Laboratory) for a critical review of the manuscript.

REFERENCES

1. J. Rotblat, in *The Acceleration of Particles to High Energies*, Institute of Physics, London, 1950, p. 54.
2. M. S. Livingston, 'High Energy Accelerator—Synchrotrocyclotron,' *Ann. Rev. Nucl. Sci.* **1**, 167 (1952).
3. H. Wade Patterson, University of California Laboratory Synchrocyclotron, in *Conference on Shielding of High-Energy Accelerators, New York, April 11–13, 1957*, TID–7545, pp. 3–7.
4. E. J. Lofgren, reported in discussion session, op. cit., Ref. 3, page 64.
5. C. E. Falk, in Introductory Remarks, op. cit., Ref. 3.
6. Preliminary conclusions of ECFA, CERN Internal Report CERN/SPC/228/Rev. 2, June 17, 1966.
7. *Proceedings Premier Colloque International sur la Protéction Auprès des Grands Accélerateurs* (Presses Universitaires de France, 108 Blvd. St. Germain, Paris, 1962).
8. *Proceedings of the USAEC First Symposium on Accelerator Radiation Dosimetry and Experience*, held at Brookhaven National Laboratory, New York, November 3–5, 1965, CONF–651109.
9. *Proceedings of the First International Symposium on the Biological Interpretation of Dose from Accelerator-Produced Radiation*, held at the Lawrence Radiation Laboratory, Berkeley, California, March 13–16, 1967, CONF–670305.
10. *Proceedings of the Conference on Radiation Protection in Accelerator Environments*, held at the Rutherford Laboratory, England, March 1969 (Rutherford Laboratory Publication).
11. *Proceedings of the Second International Conference on Accelerator Dosimetry and Experience*, held at the Stanford Linear Accelerator Center, Stanford, California, Nov. 5–7, 1969, CONF–691101.
12. S. J. Lindenbaum, 'Shielding of High Accelerators,' *Ann. Rev. Nucl. Sci.* **11**, 213 (1961).
13. M. S. Livingston and J. P. Blewett, *Particle Accelerators* (McGraw-Hill, New York, 1962).
14. M. Ladu, 'Problems of Safety and Radiation Protection Around High Energy Accelerators,' p. 365 in *Health Physics*, Ed. A. M. F. Duhamel (Pergamon Press, Oxford, 1969), Vol. 2, Part I.
15. F. P. Cowan, 'Ultra-High Energy Radiation and Uncommon Types of Particles,' in *Radiation Dosimetry*, Eds. F. H. Attix and E. Tochilin (Academic Press, New York, 1965), Vol. III.
16. J. Baarli, 'Dosimetry of Very High Radiation,' op. cit., Ref. 14, p. 291.
17. M. Barbier, *Induced Radioactivity*, (North-Holland Publishing Co., Amsterdam, 1969).
18. Engineering Compendium on Radiation Shielding (Springer-Verlag, Berlin) Vol. 1, 1968, Vol. 2, in press, Vol. 3, 1970.
19. 200 BeV Accelerator Design Study (2 vols.), Lawrence Radiation Laboratory-Berkeley UCRL–16000, June 1965.
20. Report on the Design Study of a 300 GeV Proton Synchrotron by the CERN Study Group on New Accelerators (2 vols.), CERN/563, November 1964.
21. Yale University Design Study Staff, 'A Final Report on the Design of a Very-High-Intensity Proton Linear Accelerator as a Meson Factory of 750 MeV,' Report 412, October 1964.
22. 'A Proposal for a High-Flux Meson Facility,' Los Alamos Scientific Laboratory Report, September 1964; see also D. R. F. Cochran, 'Radiation Problems Associated with the LAMPF Facility,' op. cit. Ref. 8, p. 459.
23. 'A Proposal for Increasing the Intensity of the Alternating Gradient Synchrotron at the Brookhaven National Laboratory,' BNL–7956, May 1964.
24. M. N. Chimankov *et al.*, 'Radiation Situation Around the Linac Injector of the 70 GeV Proton Synchrotron,' (preprint), Institute of High Energy Physics, Serpukhov, IHEP 69–67; V. T. Golovachik *et al.*, 'Induced Radioactivity at the IHEP Proton Synchrotron,' IHEP 69–76; V. T. Golovachik *et al.*, 'Recent Radiation Measurements at the Serpukhov Proton Synchrotron' (preprint 1970).
25. B. J. Moyer, 'Buildup Factors,' op. cit. Ref. 3, p. 96.
26. N. Metropolis *et al.*, 'Monte Carlo Calculations in Intra-Nuclear Cascades I and II,' *Phys. Rev.* **110**, 185 (1958).
27. D. H. Perkins, 'Results from Cosmic Ray Experiments in High Energy Physics Study,' Lawrence Radiation Laboratory Report UCRL–10022, 1963.
28. D. Keefe, 'μ–Meson Shielding Problems at 200 GeV: Approximate Calculations,' Lawrence Radiation Laboratory Internal Report UCID–10018, May 20, 1964.
29. B. J. Moyer, R. Hildebrand, T. J. Parmley, and H. York, 'Character of the Radiation and Shielding at the 184–Inch Cyclotron,' USAEC Document AECD–2149, 1947.
30. H. W. Patterson, 'The Effect of Shielding on Radiation Produced by the 730–MeV Synchrocyclotron and the 6.3–GeV Proton Synchrotron at the Lawrence Radiation Laboratory,' op. cit. Ref. 7, p. 95.
31. B. T. Price, C. C. Horton, and K. T. Spinney, *Radiation Shielding*, (Pergamon Press, Oxford, 1957), Chapter 4.

32. R. H. Thomas, 'The Radiation Field Observed Around High-Energy Energy Nuclear Accelerators,' in *Progress in Radiology* (Excerpta Medical Foundation, Amsterdam, 1967), Vol. 2 p. 1849.
33. P. Tardy-Joubert, 'Methods and Experience in Dosimetry at the Saturne Synchrotron,' op. cit. Ref. 8, p. 117.
34. H. W. Patterson, *et al.*, The Flux and Spectrum of Cosmic-Ray-Produced Neutrons as a Function of Altitude, *Health Phys.* **2,** 69 (1959).
35. W. N. Hess *et al.*, *Phys. Rev.* **46,** 445 (1959).
36. J. T. Routti, 'High Energy Neutron Spectroscopy with Activation Detectors,' Lawrence Radiation Laboratory Report UCRL–18514, April 1969.
37. W. S. Gilbert *et al.*, '1966 CERN-LRL-RHEL Shielding Experiment at the CERN Proton Synchrotron,' Lawrence Radiation Laboratory Report UCRL–17941, Sept. 1968.
38. R. H. Thomas, 'The Proton Synchrotron as a Source of Radiation,' op. cit. Ref. 17, Vol. 1.
39. D. Keefe and M. Scolnick, 'Table of Mean Free Path and Radiation Length for Various Materials,' Lawrence Radiation Laboratory Accelerator Study Internal Report, AS/EXP 01 Dec. 10, 1966.
40. H. de Staebler, 'Transverse Radiation Shielding for the Stanford Two-Mile Accelerator,' USAEC Report SLAC–9, Nov. 1962.
41. B. J. Moyer, 'Evaluation of Shielding Required for the Improved Bevatron,' Lawrence Radiation Laboratory Report UCRL–9769, June 1961.
42. B. J. Moyer, 'Method of Calculating the Shielding Enclosure of the Bevatron,' op. cit, Ref. 7, p. 65.
43. R. H. Thomas, 'Shield Design Examples—The Bevatron,' op. cit. Ref. 17, Vol. 2.
44. W. S. Gilbert *et al.*, '1966 CERN-LRL-RHEL Shielding Experiment at the CERN Protron Synchrotron,' Lawrence Radiation Laboratory Report UCRL–17941, Sept. 1968.
45. J. T. Routti and R. H. Thomas, 'Moyer Integrals for Estimating Shielding of High Energy Accelerators,' *Nucl. Instr. Methods* **76,** 157 (1969).
46. A. R. Smith, 'The Stray Radiation Field of the Bevatron,' Lawrence Radiation Laboratory Report UCRL–8377, 1958.
47. A. R. Smith, 'Some Experimental Shielding Studies at the 6.2–BeV Berkeley Bevatron,' op. cit. Ref. 8. p. 365.
48. A. Citron, L. Hoffmann, and C. Passow, *Nucl. Instr. Methods* **14,** 97 (1961).
49. R. H. Thomas (Editor), 'Report of the Shielding Conference held at the Rutherford Laboratory, Sept. 26, 27, 1963,' NIRL/R40.
50. L. Hoffmann, 'A Summary of the Shielding Experiments Using 20 GeV Protons of the CERN PS,' op. cit. Ref. 49. p. 3.
51. J. Geibel *et al.*, 'Shielding Studies in Steel with 10– and 20–GeV/c Protons. Part I. General Description of the Experiment,' *Nucl. Instr. Methods* **32,** 45 (1965).
52. R. L. Childers, C. D. Zerby, C. M. Fisher, and R. H. Thomas, 'Shielding Studies in Steel with 10– and 20–GeV/c Protons. Part III. Measurement of the Nuclear Cascade at 10 GeV/c with Emulsions,' *Nucl. Instr. Methods* **32,** 53 (1965).
53. A. Citron, L. Hoffmann, C. Passow, W. R. Nelson, and M. Whitehead, 'Shielding Studies in Steel with 10– and 20–GeV Protons. Part II. A Study of the Nuclear Cascade in Steel Initiated by 19.2–GeV/c Protons,' *Nucl. Instr. Methods* **32,** 48 (1965).
54. J. Baarli, K. Goebel, and A. H. Sullivan, 'Shielding Studies in Steel with 10– and 20–GeV Protons, Part IV. Measurement of the Penetration of a 10– and 19.2–GeV/c Proton Beam in Steel Using Ionization Chambers and Plastic Phophors,' *Nucl. Instr. Methods* **32,** 57 (1965).
55. S. J. Lindenbaum, quoted by J. Baarli, *et al.*, Ref. 54.
56. R. G. Alsmiller, F. S. Alsmiller, and J. E. Murphy, 'Neutron Meson Cascade Calculations: Transverse Shielding for a 45–GeV Electron Accelerator (Part I),' Oak Ridge National Laboratory Report ORNL–3289, 1962.
57. R. G. Alsmiller, F. S. Alsmiller, and F. E. Murphy, 'Neutron Meson Cascade Calculations: Transverse Shielding for a 45–GeV Electron Accelerator (Part II),' Oak Ridge National Laboratory Report ORNL–3365, 1963.
58. R. G. Alsmiller and J. E. Murphy, 'Nucleon Meson Cascade Calculations: The Star Density Produced by a 24–GeV Proton Beam in Heavy Concrete,' Oak Ridge National Laboratory Report ORNL–3367, 1963.
59. J. A. Geibel and J. Ranft, 'Shielding Studies in Steel with 10– and 20–GeV/c Protons, Part VI. Monte Carlo Calculations of Nucleon Meson Cascade in Shielding Materials,' *Nucl. Instr. Methods* **32,** 65 (1965).
60. J. Ranft, 'Improved Monte Carlo Calculation of the Nucleon-Meson Cascade in Shielding Material, I and II,' *Nucl. Instr. Methods* **48,** 133 (1967), and **48,** 261 (1967).
61. A. R. Smith, J. B. McCaslin, and M. Pick, 'Radiation Field Inside a Thick Concrete Shield for 6.2–BeV Incident Protons,' Lawrence Radiation Laboratory Report UCRL–11331, Sept. 18, 1964.
62. R. H. Thomas, 'Shielding Experiment at 6 GeV(I),' Lawrence Radiation Laboratory Internal Report UCID–10023, Feb. 28, 1964.
63. K. B. Shaw, (Rutherford Laboratory) private communication to R. H. Thomas, Ref. 62, 1964.
64. W. R. Frisken, (Brookhaven National Laboratory), private communication to W. H. Moore, Ref. 65, 1965.
65. W. H. Moore, 'Source of High-Energy Particles from an Internal Target in the AGS,' Brookhaven National Laboratory Report AGSCD–62, Jan. 24, 1966.
66. L. Hoffmann and A. H. Sullivan, 'Studies of the Shielding Required for the Secondary Radiation Produced By a Target in a High-Energy Proton Beam. V: Studies of the Shielding,' *Nucl. Instr. Methods* **32,** 61–64 (1965).
67. S. J. Charalambus, K. Goebel, and D. Nachtigall, 'Angular Distribution of Secondary Particles and Dose Rates Produced by 19.2–GeV/c Protons Bombarding Thin Be, Al, Cu, and U Targets,' CERN DI/HP, March 14, 1967.
68. N. R. Casey, C. H. Distenfeld, G. S. Levine, W. H. Moore, and L. W. Smith, 'Sand as a Side Shield for 30–GeV Protons Stopping in the Brookhaven AGS,' *Nucl. Instr. Methods* **55,** 253 (1967).
69. K. O'Brien and J. McLaughlin, 'Propagation of the Neutron Component of the Nucleon Cascade at Energies Less Than 500 MeV: Theory and a Solution

to the Accelerator Transverse Shielding Problem,' *Nucl. Instr. Methods* **60,** 129 (1968).
70. B. Davidson, *Neutron Transport Theory* (Oxford, 1967).
71. C. Distenfeld and D. Colvett, *Nucl. Sci. Eng.* **26,** 117 (1966).
72. K. O'Brien and J. E. McLaughlin, 'Calculation of Dose and Dose-Equivalent Rates to Man in the Atmosphere From Galactic Cosmic Rays,' HASL Report HASL–228, May 1970.
73. W. S. Gilbert, 'Radiation Problems with High Energy Proton Accelerators,' in *Proceedings of the 1967 U.S. National Particle Accelerator Conference, Washington, D.C., March 1–3, 1967,* IEEE *Trans. Nucl. Sci.* **NS–14,** No. 3, 965 (1967).
74. R. D. Fortune, W. S. Gilbert, and R. H. Thomas, 'Shielding Experiment at the CERN PS,' Lawrence Radiation Laboratory Internal Report UCID–10199, April 28, 1967.
75. W. S. Gilbert, 'Beam Loss and Shielding Experiment, in *Proceedings of the Sixth International Conference on High Energy Accelerators, Cambridge, Mass., Sept. 11–15, 1967.* p. 221.
76. W. S. Gilbert, 'Shielding Measurements of the CERN 25–GeV Proton Synchrotron,' op. cit. Ref. 11, p. 323.
77. M. Awschalom *et al.*, Design Report, National Accelerator Laboratory, July 1968, Chapt. 12, 'Radiation and Shielding,' p. 7–8.
78. M. Awschalom, 'Lateral Shielding for the 8–GeV and 200–GeV Synchrotrons,' National Accelerator Laboratory Internal Report TM–241, May 25, 1970.
79. J. Ranft, 'Monte Carlo Calculation of Particle Loss Distribution Along the Vacuum Chamber of the CPS Near Internal Targets and of the Transverse Attenuation of Strongly Interacting Particle Fluxes in the PS Magnet Units and Earth Shield,' CERN Internal Report MPS/INT. MU/EP 67–5, June 20, 1967.
80. J. Ranft, 'Improved Monte Carlo Calculation of the Nucleon-Meson Cascade in Shielding Material. I. Description of the Method of Calculation,' *Nucl. Instr. Methods* **48,** 133 (1967).
81. J. T. Routti and R. H. Thomas, 'Angular Distribution of Secondary Neutrons and Protons from High Energy Interactions,' in preparation; also see Gilbert *et al.*, Ref. (44).
82. E. Close, 'FLUXFT–A CDC 6600 Code for Fitting Radiation Data Associated with the CERN–PS,' Lawrence Radiation Laboratory Internal Report UCID–3061, July 1967.
83. G. S. Levine and W. H. Moore, 'Beam Stop Studies at the Brookhaven AGS,' in *Proceedings of the Second International Conference on Accelerator Dosimetry and Experience. Stanford, California, November 5–7, 1969,* CONF–691101.
84. G. S. Levine and W. H. Moore, 'Beam Stop for 28–GeV/c Protons,' in *Proceedings of the Second International Conference on Accelerator Dosimetry and Experience held at Stanford, California, November 5–7, 1969,* CONF–691101.
85. K. Goebel and J. Ranft, 'Radiation Measurements Around a Beam Stopper Irradiated by 19.2–GeV/c Protons and Neutron Energy Spectra by Monte Carlo Nucleon-Meson Cascade Calculations,' in *Proceedings of the Second International Conference on Accelerator Dosimetry and Experience held at Stanford, California, November 5–7, 1969,* CONF–691101.
86. R. A. Andrews *et al.*, 'Design of the 200 GeV Slow Extracted Beam at NAL,' National Accelerator Laboratory Internal Note C26, 1969.
87. G. Wheeler, (Brookhaven National Laboratory), private communication, 1970.
88. S. J. Lindenbaum, op. cit. Ref. 3.
89. C. Distenfeld and R. Colvett, 'Alternating Gradient Synchrotron Conversion Summary,' in *Proceedings of the First Symposium on Accelerator Radiation Dosimetry and Experience, Brookhaven National Laboratory, November 3–5, 1965,* CONF–651109
90. R. G. Alsmiller *et al.*, 'The Lateral Spread of High Energy ($\leq$400 MeV) Neutron Beams and Earthshine,' Oak Ridge National Laboratory ORNL–TM–3025 August 3, 1970.
91. R. G. Alsmiller, M. Leimdorfer, and J. Barish, 'High Energy Meson Transport and the Muon Backstop for a 200 GeV Proton Accelerator,' Oak Ridge National Laboratory ORNL–4322, Nov. 68.
92. R. G. Alsmiller and J. Barish, 'High Energy Muon Transport and the Muon Backstop for a Multi-GeV Proton Accelerator,' Oak Ridge National Laboratory ORNL–4386, March 1969.
93. D. Theriot, 'Muon dE/dx and Range Tables: Preliminary Results for Shielding Materials,' National Accelerator Laboratory Internal Report TM–229, March, 30 1970.
94. D. Theriot and M. Awschalom, 'Muon Shielding—Design Studies of Homogeneous Soil Shields at 200 GeV,' National Accelerator Laboratory Internal Report TM–245, May 14, 1970.
95. R. H. Thomas, 'Energy Loss of High Energy Muons,' Lawrence Radiation Laboratory Internal Report UCID–10010, July 2, 1964.
96. D. Keefe and M. Scolnick, 'Trapping of μ–Mesons in Magnet Structure,' Lawrence Radiation Laboratory Internal Report UCID–10163, Sept. 13, 1965.
97. D. Keefe and C. Noble, 'Radiation Shielding for High Energy Muons,' Lawrence Radiation Laboratory Report UCRL–18117, March 1968.

Received 28 December 1970.